CESRL REPORT NO. 78-2
SEPTEMBER 1978

DEVELOPMENT OF LOADING SYSTEM AND INITIAL TESTS—SHORT COLUMNS UNDER BIDIRECTIONAL LOADING

by

J. O. JIRSA,
K. MARUYAMA
AND
R. RAMIREZ

Final Report on a Research Project
Sponsored by
National Science Foundation
Research Applied to National Needs Program
Grant No. ENV75-00192

DEPARTMENT OF CIVIL ENGINEERING / Structures Research Laboratory
THE UNIVERSITY OF TEXAS, AUSTIN, TEXAS

DEVELOPMENT OF LOADING SYSTEMS AND INITIAL TESTS--SHORT COLUMNS UNDER BIDIRECTIONAL LOADING

by

J. O. Jirsa, K. Maruyama, and H. Ramirez

Final Report on a Research Project

Sponsored by

National Science Foundation
Research Applied to National Needs Program
Grant No. ENV75-00192

CESRL Report No. 78-2

Civil Engineering Structures Research Laboratory
Department of Civil Engineering
The University of Texas at Austin

September 1978

C O N T E N T S

F I G U R E S

CHAPTER 1

INTRODUCTION

In recent years, the influence of bidirectional ground motion on the performance of structures has been questioned. Major earthquakes, especially the Tokachi-Oki earthquake in 1968 and the San Fernando earthquake in 1971 motivated structural engineers to study the behavior of structures and members under multidirectional load reversals [1,2,3,4,5]

In the design of structures for lateral loads, it is generally assumed that the direction of deformation coincides with a principal axis of the structure or member and with constant axial (generally compressive) forces on the columns. However, this design procedure may not be safe. Some columns designed using these assumptions suffered serious damage during earthquakes. The observed damage may be partially attributed to multidirectional forces during the earthquake.

In the design of reinforced concrete columns, the concept of biaxial bending (primarily eccentric loading on long columns) was first introduced in the 1950's [6,7]. Design criteria for biaxial bending are now well-developed. However, the loading considered in the development of such design criteria was static loading to failure, not cyclic load reversals in the inelastic range.

Post-earthquake observations have indicated that most severe damage was due to instability of columns under large deformation and shear distress of short columns. Because of the damage observed, designers and researchers have been reevaluating design criteria and initiating new programs to investigate the behavior of structures under multidirectional cyclic loading in the inelastic range.

In studies of long columns in which the flexural mode of failure dominates, the use of moment-curvature relationships has been elaborated

to explain the flexural characteristics of reinforced concrete columns subjected to load reversals in the inelastic range. Behavioral models have been developed, including bilinear and trilinear models and models with degrading stiffness. Morever, this concept has been extended into two-directional models by analogy with plastic theory [8,9]. These models appear to correlate well with experimental results in which biaxial bending due to bidirectional lateral load as well as eccentric load on columns has been studied [10,11,12,13].

On the other hand, very few studies have been conducted on reinforced concrete columns failing in a shear mode. Analytically, the most difficult problem is the mathematical description of the behavior of members after the initiation of shear cracks. It may be considered that the shear resistance after shear cracks form is due to aggregate interlock, dowel action of longitudinal reinforcement, and the confinement effect of transverse reinforcement [14]. The shear friction concept was introduced by Mattock [14,15] to examine the role of transverse reinforcement on the ultimate shear strength of reinforced concrete. However, no effective method has yet been established for treating shear behavior in a manner such as the moment-curvature concept for flexural behavior.

The Building Research Institute of the Ministry of Construction in Japan has conducted a very large and well-organized project concerned with the shear behavior of reinforced concrete short columns under unilateral inelastic load reversals. This project was conducted over a five-year period (1973-1977) and about four hundred specimens were tested. Many parameters which were considered to influence the behavior of columns were examined [16].

1.1 Objectives of Overall Project

A review of the literature shows that very few data are available regarding the shear behavior and design of reinforced concrete frames subjected to bidirectional loadings. To understand better the shear behavior of columns and joints in reinforced concrete frames, a major

research program has been initiated at The University of Texas at Austin. The objectives of the research program are as follows:

(1) To evaluate the importance of load history (bidirectional lateral loads and varying axial load levels) on the response of columns and beam-column joints of reinforced concrete structures. The prime variable to be considered is the sequence of application of lateral movements and axial forces.

(2) To develop design recommendations for the shear strength of columns and beam-column joints under skewed lateral loads or deformations and various levels of axial load.

(3) To develop models which can be used to predict the behavior of columns and beam-column joints subjected to large shear forces.

1.2 Object of Report

The object of this report is to describe the special loading facilities developed for the application of bidirectional lateral loads and varying axial loads (tension and/or compression) on short columns failing in shear. The design of the specimen is discussed and the instrumentation used to monitor the behavior is described. Finally, the results of four test specimens are presented to give an indication of the capabilities of the loading and data acquisition systems developed.

1.3 Acknowledgments

The development of the bidirectional loading facility was supported by the Division of Advanced Environmental Research and Technology of the National Science Foundation's Research Applied to National Needs Program under Grant No. ENV75-00192. With this support a floor-wall reaction system was constructed. A system for applying bidirectional lateral load using a servo-controlled hydraulic actuator was developed. The loading and data acquisition are computer-controlled.

Under Grant No. ENV75-00192, testing of short columns was initiated. Funding for a comprehensive test program on columns and beam-column joints failing in shear has been received (Grant No. ENV77-20816). The grant will provide funding for extensive experimental work, data reduction and

evaluation aimed toward establishing behavior models, and development of design recommendations for frame structures subjected to bidirectional deformations.

The project has had the guidance and input of an Advisory Panel consisting of the following:

Professor V. V. Bertero, University of California, Berkeley
Dr. W. G. Corley, Portland Cement Association, Skokie, Illinois
Mr. James Lefter, Veterans Administration, Washington, D.C.
Mr. C. W. Pinkham, S. B. Barnes & Associates, Los Angeles, California
Mr. L. A. Wyllie, Jr., H. J. Degenkolb & Associates, San Francisco, California

The assistance of the Advisory Panel and the National Science Foundation Program Manager, Dr. John B. Scalzi, is gratefully acknowledged.

The project has been conducted at the Civil Engineering Structures Research Laboratory at Balcones Research Center of The University of Texas at Austin. The Laboratory is under the direction of Dr. John E. Breen. The project is under the direction of Dr. J. O. Jirsa. Faculty associates include Dr. J. E. Breen, Dr. R. E. Klingner, and Dr. J. A. Yura. The authors wish to acknowledge the support of the laboratory staff, George E. Moden, Dan Perez, David Marschall, Gorham Hinckley, Joe Longwell, Larry Johnson, and David Stolle, who assisted in the construction of facilities and in the initial testing.

CHAPTER 2

COLUMN TEST SPECIMEN

2.1 Design Requirements

The objective of the program was to examine the behavior of reinforced concrete columns failing in shear. Therefore, it was necessary to design a test specimen with a short stiff column. In addition, the specimen was to be subjected to axial tensile or compressive loadings. Based on these requirements, the specimen selected was a short column element framing into enlarged end blocks which could be attached to a load frame. The loading frame was designed to restrain rotation of the end blocks. As a result, the specimen could be considered to simulate a short column framing into a relatively stiff floor system.

The prototype column was designed as an 18 in. square section meeting the requirements of ACI 318-77 [17]. Because the fabrication cost of the load frame required to test the large section was excessive, the test specimen was scaled to produce a column section which could be conveniently and economically tested and which would permit the use of available reinforcing bar sizes.

2.2 Specimen Details

Column Section. The test specimen is shown in Fig. 2.1. The specimen is a 2/3 scale model of an 18 in. (46 cm) square section with eight #9 (28mm) longitudinal bars ($\rho_g = 0.025$). For the transverse reinforcement, #3 bars were used. Cover in the prototype was 1-1/2 in. (3.8 cm). With the 2/3 scale factor, #6 (19 mm) longitudinal bars were used and cover was reduced to 1 in. (2.5 cm). For transverse reinforcement, special 6 mm (#2) deformed bars were obtained. All reinforcement was Grade 60.

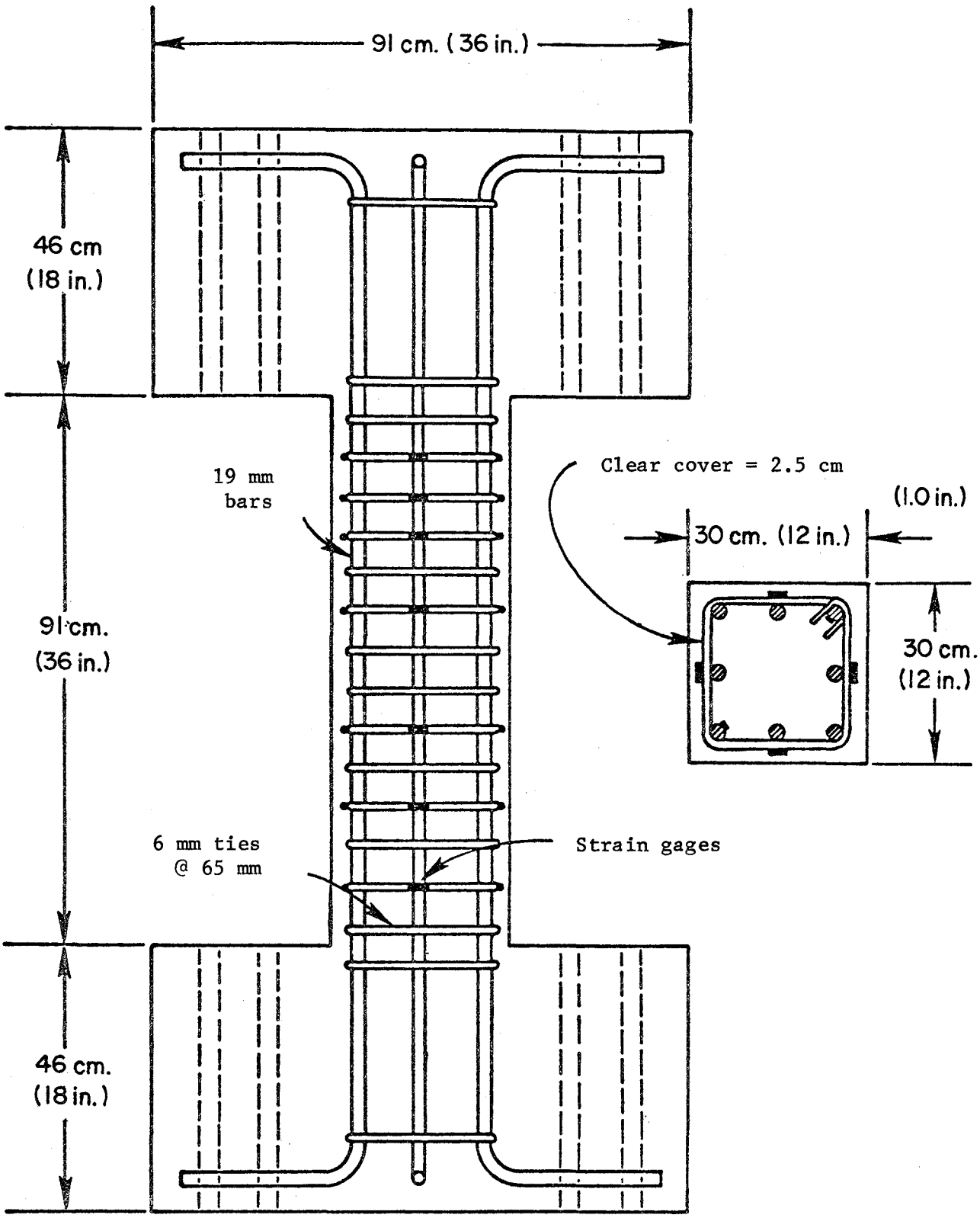

Fig. 2.1 Test specimen

Transverse Reinforcement. The spacing of the transverse reinforcement was critical if a shear mode of failure was to be obtained. It was necessary to select a spacing which would typify a column section but would not have sufficient transverse reinforcement to preclude a shear failure. Using ACI 318-77, the required shear reinforcement can be determined using

$$A_v = (v_u - v_c)b_w s/f_y$$

With f_y = 60 ksi (414 MPa) and f'_c = 5 ksi (35 MPa), the calculated maximum moment of the column section (with no axial load) is about 970 in.-k (110 kN-M). To develop maximum moment at both ends of a column 36 in. long (91 mm), the shear force on the column section is about 54k (240 kN). Using ACI 318-77, Chapter 11, the required spacing of stirrup ties in the column is 1.7 in. (4.3 cm). It should be remembered that a spacing of 1.7 in. is required if shear failure is to be avoided.

Appendix A (Seismic Design) of ACI 318-77 also specifies confinement reinforcement to be continued into the column from the ends. For columns with low axial load ($\leq$ 0.4 balance load), the column should be designed as a flexural member with the spacing not exceeding d/4 within a distance equal to four times the effective column depth from the end of the member (Secs. A.5.9 and A.6.3). If the axial load is greater than 0.4 balance load (Sec. A.6.4), confining reinforcement (Eq. A-4) is to be supplied above and below connections over a minimum length from the face of the connection at least equal to the overall depth (larger dimension in a rectangular column), 18 in. or 1/6 the clear height of the column. The maximum spacing for the confining hoops is 4 in. (10 cm) or 2.7 in. (6.7 cm) in a 2/3 scale model. Using Sec. A.6.4, the required spacing is 2.4 in. (6 cm) and using Sec. A.6.3 (d/4), the spacing is 2.59 in. (6.6 cm).

Based on the requirements that the columns should fail in shear and also that the transverse reinforcement should be typical for a moment-resisting frame structure, the spacing of stirrup ties was set at 2.5 in. (6.5 cm).

End Block. In the specimens, the dimensions of the end blocks were based on the area needed to attach the column to the test frame and the depth needed to adequately anchor the column longitudinal bars.

It was decided to attach the specimen to the frame with eight high strength bolts at each end of the column. Holes were preformed with PVC tubing (Fig. 2.2) in the end blocks with the holes located along the diagonals to the corner of the end block. With a 12 in. column section, an end block dimension of 36 in. (91 cm) permitted the use of a 12 in. square bearing plate on the surface of the end block against which the bolts could be tightened.

For the #6 column bars, the required anchorage length (using ACI 318, Chapter 12) necessitated an end block depth of about 12 in. In order to further diminish the possibility of anchorage problems and to provide an end block of sufficient rigidity, an 18 in. (46 cm) depth was chosen. Figure 2.1 shows the dimensions of the end block and Fig. 2.3 shows the specimen in place in the test frame with the end bolts and bearing plates in place.

Supplementary transverse reinforcement was included in the end block to ensure continuity should shear or flexural cracking take place under large lateral and axial loads or under cyclic reversals. The supplementary steel is shown in Figs. 2.2 and 2.4.

2.3 Formwork

The requirements for the formwork were (1) the forms were to be reusable for a number of castings and (2) the entire specimen was to be cast monolithically in one operation. Forms were constructed with a frame of steel angles to support the upper end block during casting and to provide better dimensional control. A schematic view is shown in Fig. 2.5 and a photo of the assembled forms is shown in Fig. 2.6. Openings in the bottom end block were needed to ensure proper compaction of concrete. Concrete was placed through the column to the bottom end block. When the bottom block was in place, the openings were sealed.

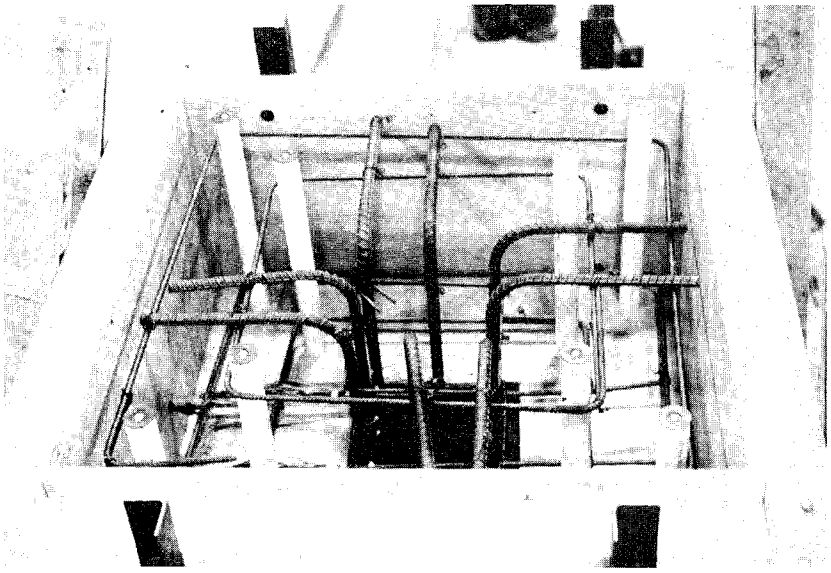

Fig. 2.2 End block reinforcement

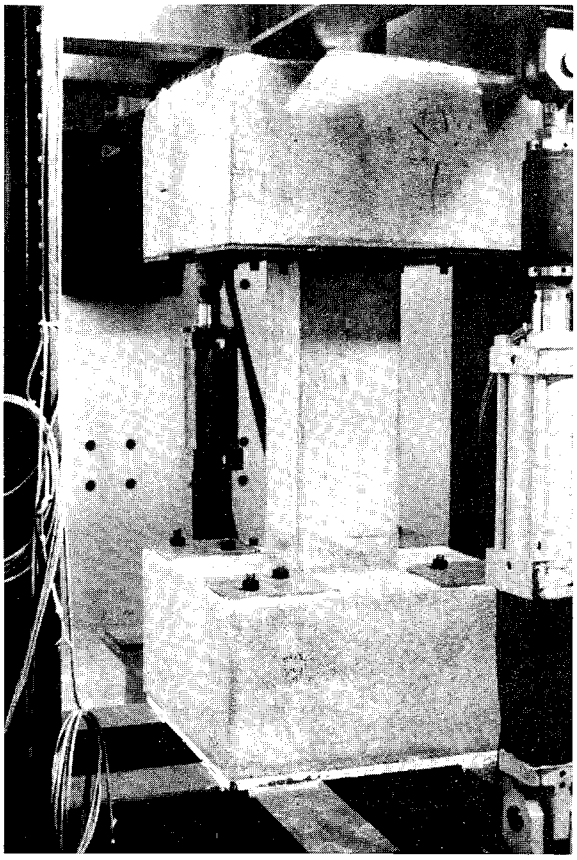

Fig. 2.3 Test specimen in place

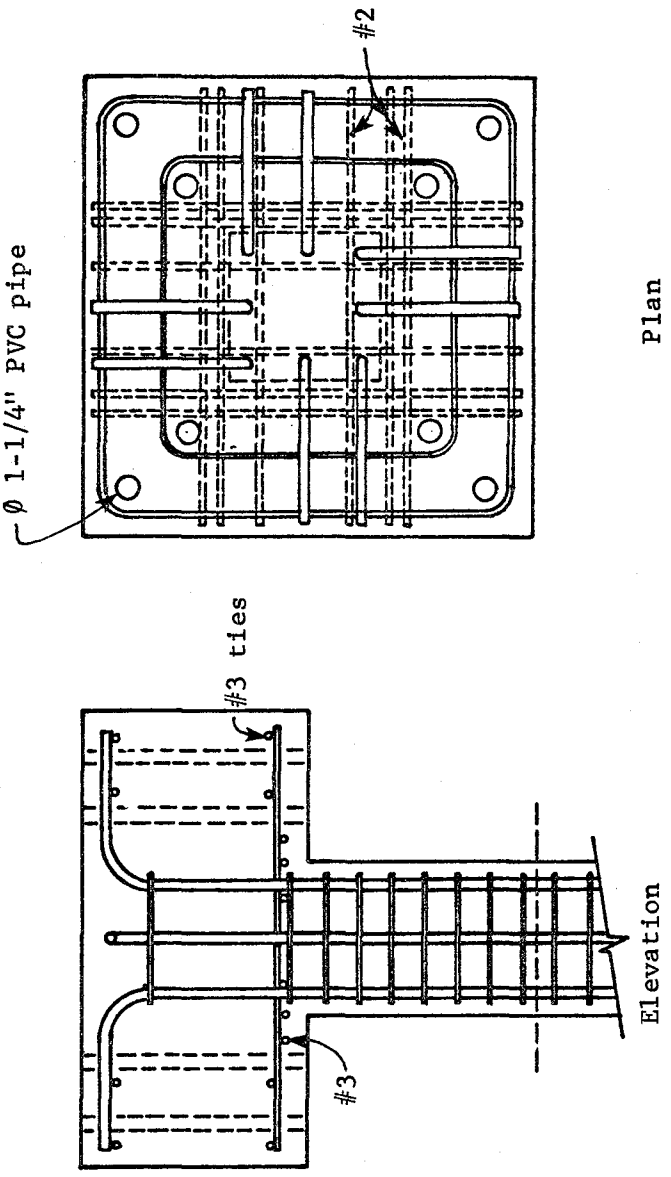

Fig. 2.4 End block details

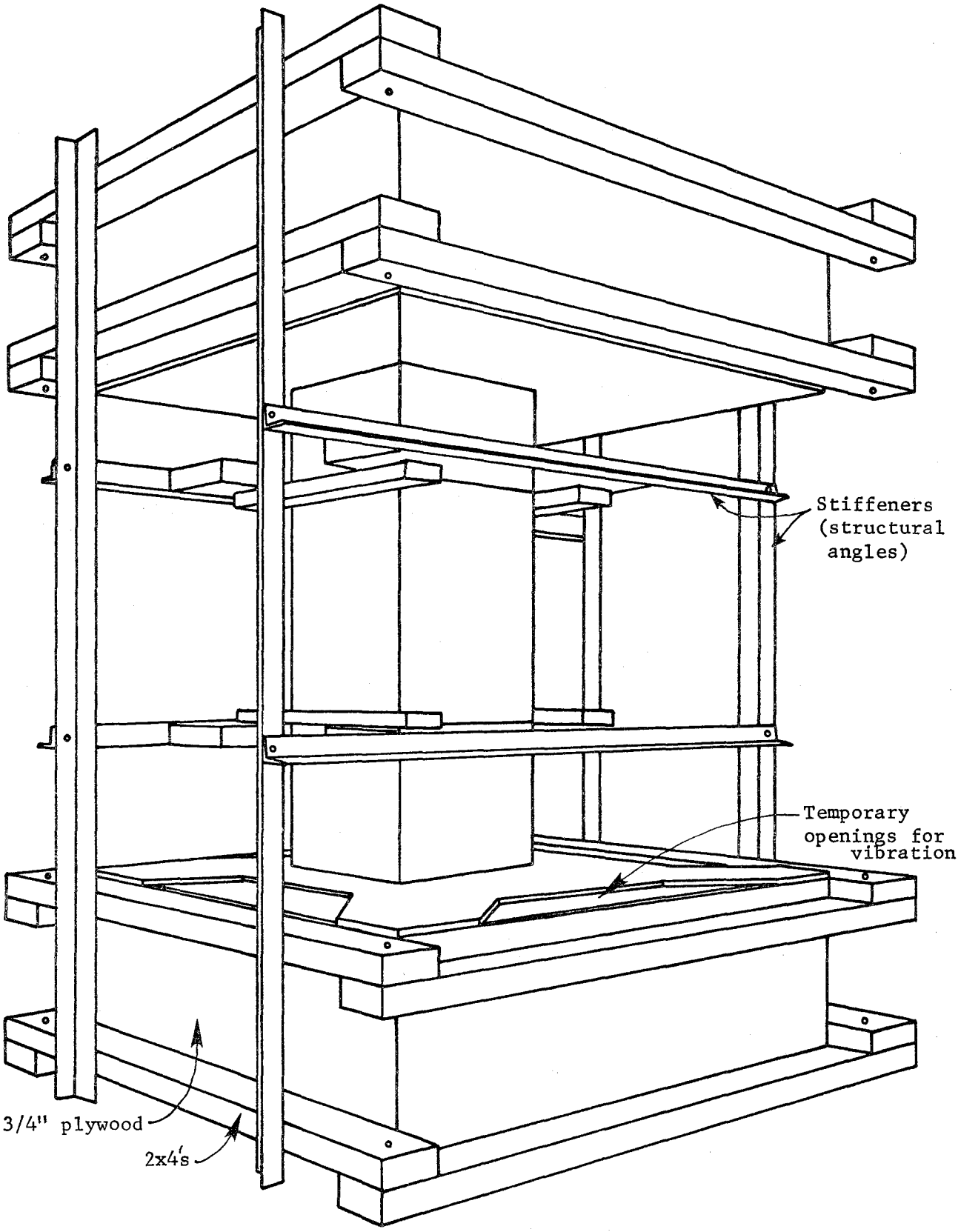

Fig. 2.5 Formwork assembly

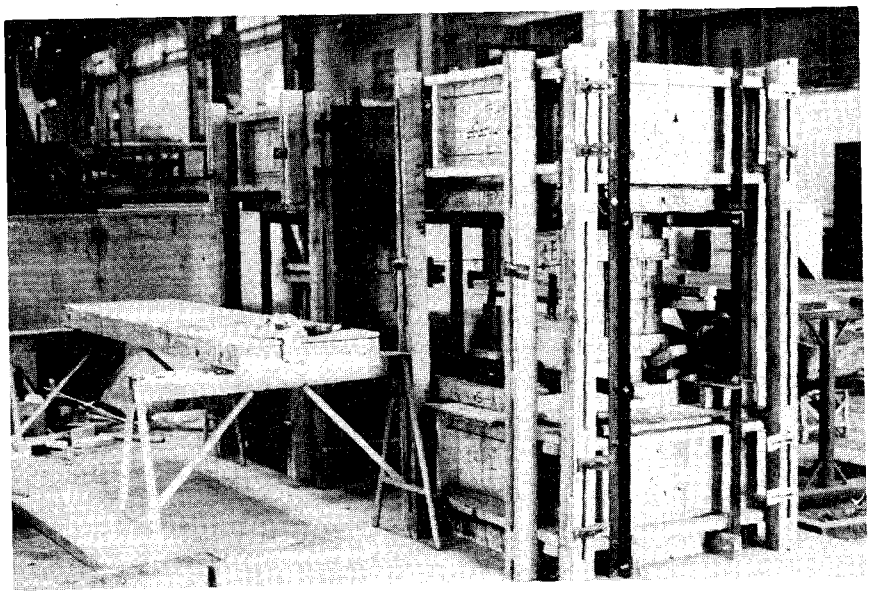

Fig. 2.6 Forms ready for casting

2.4 Materials

Concrete. Ready-mix concrete was obtained from a commercial supplier located near the laboratory. The mix proportions were as follows:

Concrete Mix Design (5000 psi, 35 MPa)

Proportions for 1 yd^3

Water	312 lb	} w/c = 0.6
Cement	520 lb	}
Fine aggregate	2200 lb	
Coarse aggregate (3/8 in.)	3240 lb	
Airsene (plasticizer)	25 oz	

The aggregate was Colorado River sand and gravel. Some of the water was withheld at the plant and adjusted at the laboratory to achieve the desired slump (6 in.). Twelve control cylinders were cast with each batch and cured with the specimens. Two specimens were cast in each operation. The forms were stripped two to three days after casting. Concrete strengths at the time of testing ranged from 4.4 to 6.0 ksi.

Reinforcement. Grade 60, #6 (19 mm) deformed bars were used for longitudinal reinforcement and Grade 60, #2 (6 mm) deformed bars for transverse reinforcement. The #2 deformed bars for all specimens were from the same shipment. The #6 deformed bars came from two different shipments. Coupons of the deformed bars were tested to obtain the modulus, yield, and ultimate for the steel. Stress-strain curves for the reinforcement are shown in Fig. 2.7

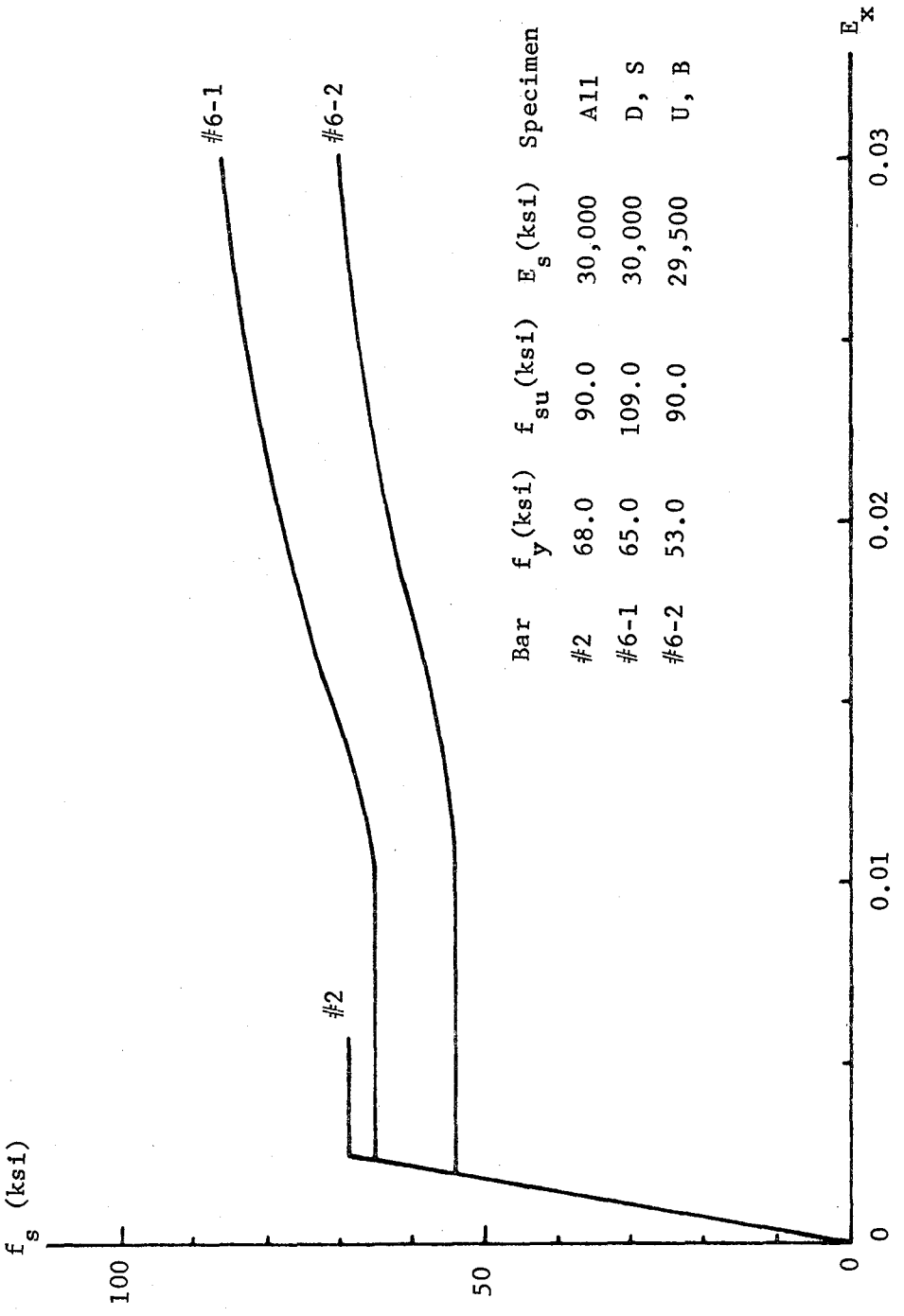

Fig. 2.7 Stress-strain curves for reinforcement

CHAPTER 3

LOADING SYSTEM

3.1 Introduction

Because of the complexity of the loading histories to be studied, it was necessary to develop a loading system which was capable of applying lateral loads independently in two lateral directions and vertical loads with a range varying from tension through compression. The lateral loads had to be applied through fairly large deformations. To reduce the complexity of the loading frame, a structural floor-wall reaction system was designed and built in the Civil Engineering Structures Research Laboratory. The floor-wall system is described in detail in Ref. 18.

3.2 Design Considerations for Test Frame

The specimen is intended to simulate a short column located between stiff floor elements. Under lateral load the rotation at the ends of such a column will be small and the column ends will be fixed while undergoing lateral translation. It is also necessary to restrain the ends so that rotation in a horizontal plane at the ends is eliminated. Several possible systems were considered before a final design was completed.

3.3 Analytical Comparisons of Test Frame Configurations

Mechanical Positioning System. The loading apparatus shown in Fig. 3.1 was developed by the Building Research Institute, Ministry of Construction in Japan [16] and has been used for studying the behavior under unilateral load reversals of reinforced concrete short columns with dimensions similar to columns in this program.

A modification of that loading frame was considered for bilateral loading. However, the positioning device takes a great deal of space,

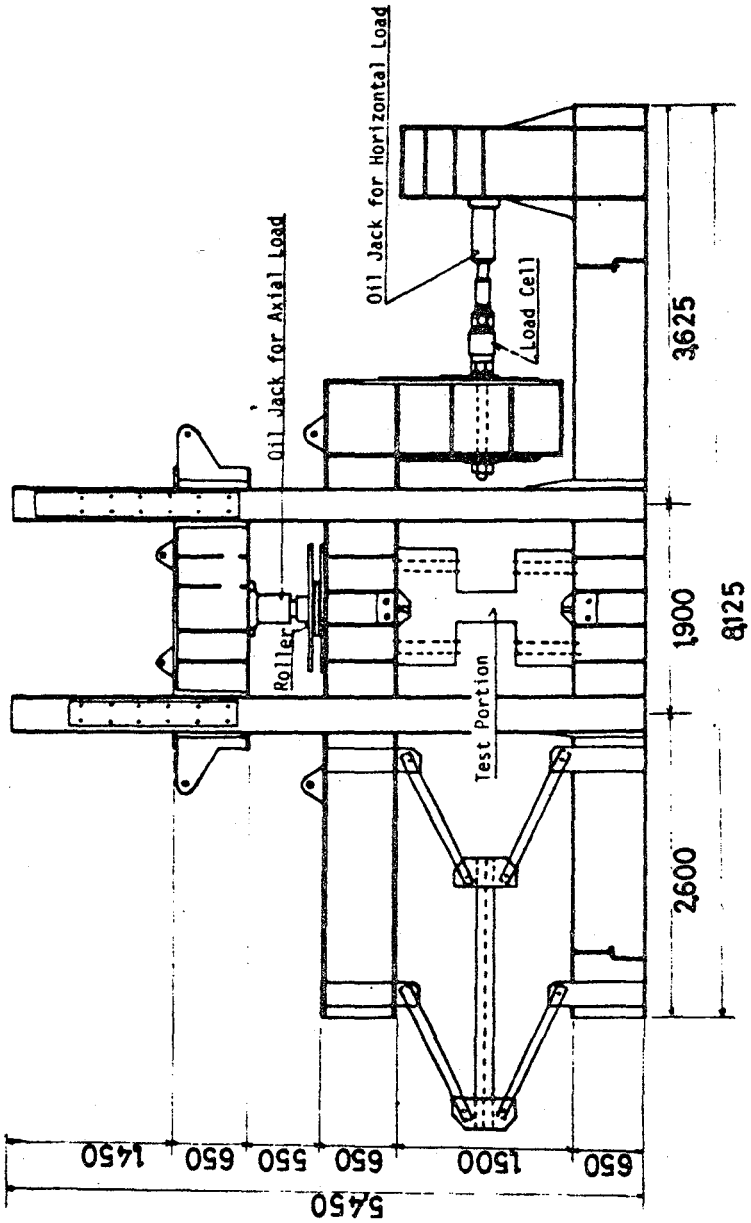

Fig. 3.1 B.R.I. loading apparatus

especially in the case of bilateral loading where a positioning apparatus is needed in two directions, as well as in the horizontal plane. Because articulations in two directions were required, the mechanical system became complex and uneconomical. To compare different systems, the stiffness of the mechanical device was calculated using a simple truss model shown in Fig. 3.2. With use of the stiffness method or flexibility method, the system stiffness can be defined. It was assumed that the large cross beam was stiff in comparison with the mechanical linkages.

Hydraulic Positioning System. To accomplish the aim of restraining rotation, but not translation, in three orthogonal planes, a system comprised of hydraulic actuators was devised. A schematic representation is shown in Fig. 3.3. With the use of double-rodded hydraulic actuators and the chambers of the actuators cross-coupled, the loading head can translate but rotation is prevented. Swivel heads at both ends permit articulation in any direction. An identical positioning system in the orthogonal vertical plane and a third pair of actuators (smaller in capacity) provide the positioning required in the horizontal plane. A calculation of the stiffness of a hydraulic actuator indicated that with a 20 $in.^2$ cross section, 6 in. chamber length, and fluid bulk modulus of oil of 200 ksi, the stiffness of the hydraulic system was very similar to the mechanical system.

3.4 Design of Loading Frame

In order to determine the final dimension of the loading frame and positioning system, the influence of the various elements of the system on the rotation of the column head was examined. A schematic view of the hydraulic positioning system is shown in Fig. 3.3 and the simple model used for analysis is shown in Fig. 3.4. Equilibrium and compatibility relationships of portions of the system are also shown in Fig. 3.4. The relationship between the force in the actuator and the column head rotation is derived as is the relationship between the external moment and the column head rotation.

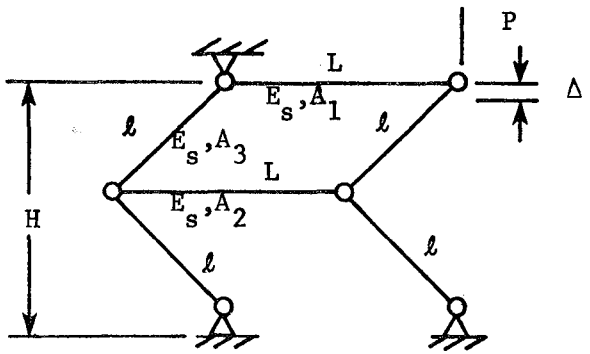

Assume $A_1 \gg A_2, A_3$

System stiffness: K

$$P = K \cdot \Delta$$

$$K = \frac{H^2}{16\ell^2 \left\{ \frac{\ell}{E_s A_3} + \frac{L}{E_s A_2} \left(1 - \frac{H^2}{4\ell^2}\right) \right\}}$$

H = height = 150 cm (60 in.)
ℓ = diagonal arm length = 120 cm (47 in.)
L = horizontal arm length = 200 cm (80 in.)
A_2 = area of horizontal arm = 56 cm^2 (8.7 in^2)
A_3 = area of diagonal arm = 4.1 cm^2 (6.3 in^2)
E_s = 200 x 10^3 MPa = 29 x 10^3 ksi
K = 400 kN/cm (230 k/in.)

Fig. 3.2 Analysis of mechanical system

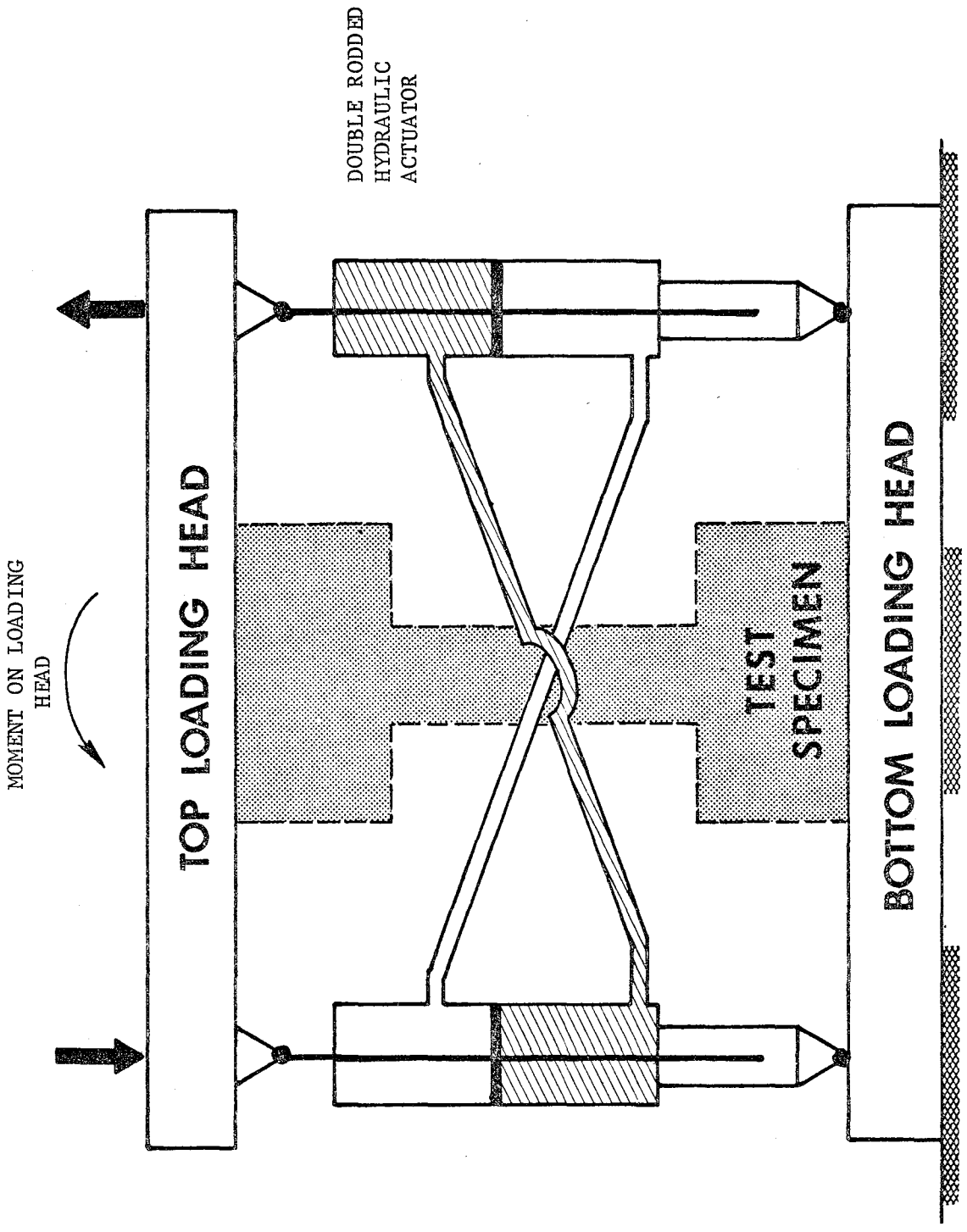

Fig. 3.3 Vertical and horizontal positioning systems

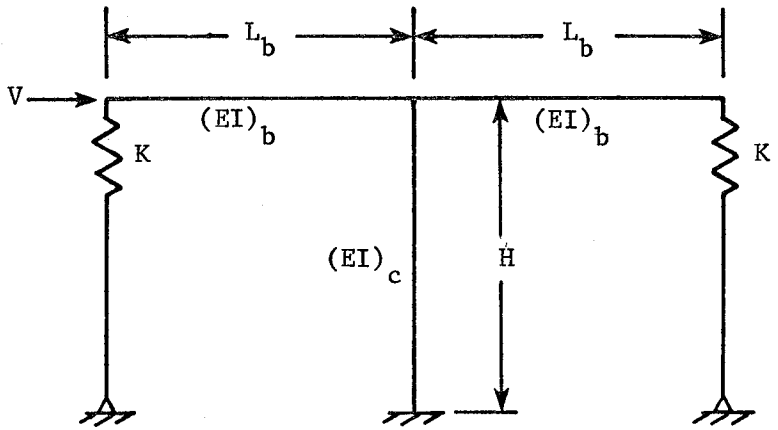

(a) Conceptual Model

Equilibrium: $M = M_c + 2L_bR$

$M_c = 4(EI)_c\theta/H$

$R = K\ \Delta$

$K = \dfrac{2A_{cy}^2}{v}$

Compatibility: $\Delta = \Delta_1 - \Delta_2$

$\Delta_1 = L_b\theta$

$\Delta_2 = RL_b^3/3(EI)_b$

Combining Equations:

$$R = L_b\theta/\left(\frac{1}{K} + \frac{L_b^3}{3(EI)_b}\right)$$

$$M = \left(\frac{4(EI)_c}{H} + \frac{2L_b^2}{\frac{1}{K} + \frac{L_b^3}{3(EI)_b}}\right)\theta$$

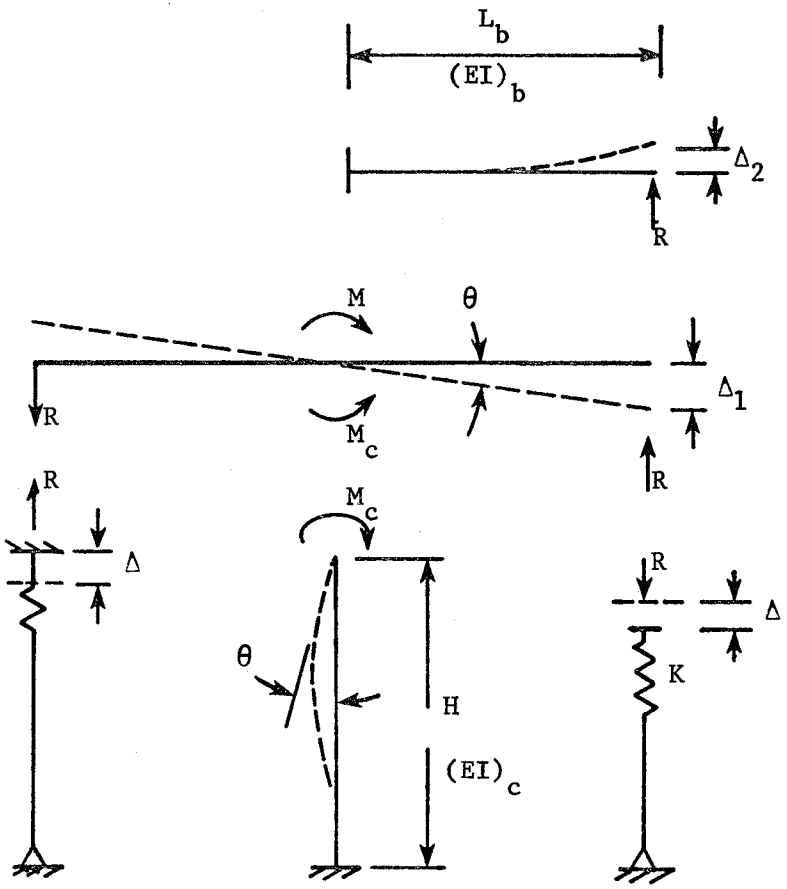

(b) Freebodies

A_{cy} = area of cylinder piston

v = volume of oil in cylinder end hoses

K_o = fluid bulk modulus of oil

Fig. 3.4 Hydraulic positioning system analysis

Using the analogy shown in Fig. 3.4, the system was studied by varying systematically the parameters which governed the stiffness. Of prime interest was the loading frame length and moment of inertia (L_b and I_b) and the area and length of the actuator chamber (A_{cy} and ℓ_{cy}). The study indicated that a 4 ft. frame length could be used; there was little improvement in the stiffness of the system if a 6 or 8 ft. length (values compatible with floor anchors) was considered. A moment of inertia of 1000 in.^{4} gave acceptable results; an increase beyond that value changed the stiffness of the system very slightly. The actuator size was shown to be an important concern and it was desirable to keep the volume of oil to a minimum by having a short stroke and to also keep the pressure differential small with a large area of piston. The analyses showed that a stroke length up to 12 in. was acceptable and an effective ram area of 20 to 40 in.^{2} was preferable. Based on these studies, the actuators and loading frame dimensions were selected.

It is interesting to note that the stiffness of the system was reasonably well predicted. Figure 3.5 shows a comparison of calculated versus test results for one specimen. Figure 3.5a shows the relationship between the ratio of calculated column moment to the moment if the end is fully fixed and the measured relationship between the measured strains in the longitudinal column reinforcement at the top and bottom ends of the column. It should be noted that the column develops yielding at both ends with a lateral deformation of about 0.4 in. Calculated values show a high ratio throughout. The differences are likely due to tolerances in fittings and seating of the specimen which produce deformation at early stages of loading. Figure 3.5b shows a comparison of measured and calculated rotation of the loading head on the top end block of the specimen. Note that the measured values are larger throughout the loading range. This is likely the result of elongations in the high-strength bolts which were used to attach the specimen to the load frame, but which were not considered in the analytical study.

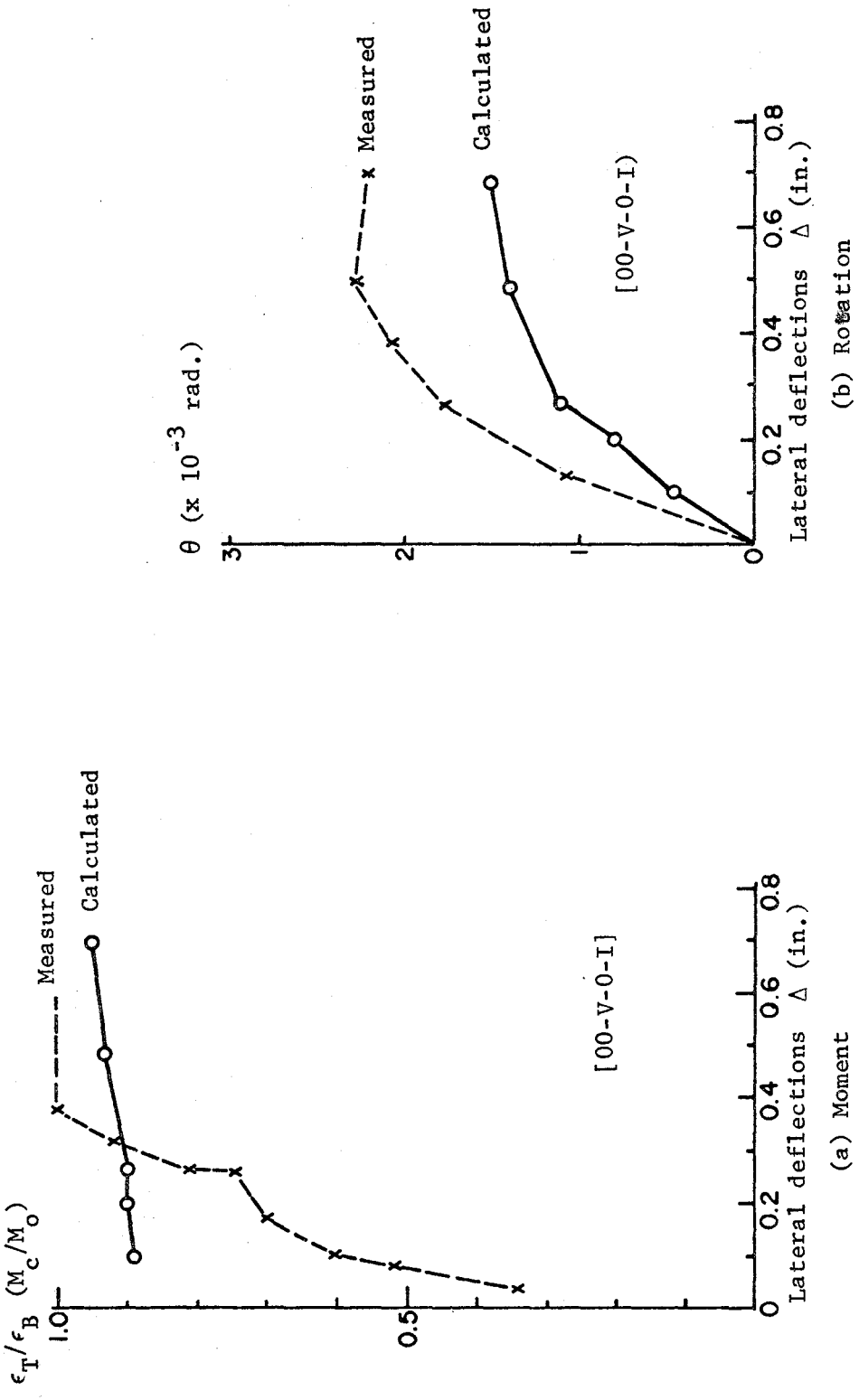

Fig. 3.5 Comparison of calculations with test results

3.5 Test Frame Details

After selection of the hydraulic positioning system had been made, the frame was designed in detail to meet the limitations imposed by the geometry of the floor-wall reaction system, the hydraulic loading and positioning system, and the specimen geometry and capacity. Figure 3.6 shows a view of the test setup. Figures 3.7 and 3.8 show elevation and plan views of the test setup.

Figure 3.9 is a schematic view of the setup without the hydraulic positioning system in place. The specimen is placed between two fabricated steel elements. The bottom element or loading base is attached directly to the laboratory floor and supports the test specimen and the ends of the vertical positioning actuator. Axial and lateral loads on the column are transferred to the floor through the loading base, which is connected to the floor with 20 high-strength anchor bolts located at the ends of the cruciform and at the center. Details of the loading base are shown in Fig. 3.10. Note that the base is detailed to utilize the anchor bolt modules (4 bolt groups on 4 ft. centers) of the permanent strong floor.

The loading head is nearly identical to the loading base, as can be seen in Fig. 3.11. The loading head supports the top ends of the vertical positioning actuators, the ends of the horizontal positioning actuators, and the ends of the lateral and axial load actuators. The central core of the loading head is stiffened to permit transfer of axial tension or compression to the column. Note that both the loading base and loading head include holes for receiving the eight high-strength bolts used to fasten the specimen to the load frame.

The loading base and head are fabricated of A36 steel. Each arm consisted of two W12x53 rolled sections which provide a moment of inertia of 852 $in.^4$, as required by the analytical study of the loading frame. All plates and wide flanges are welded to form a rigid element.

The axial load reaction is transferred to the floor through a frame made of four wide flange columns which are anchored to the floor. The

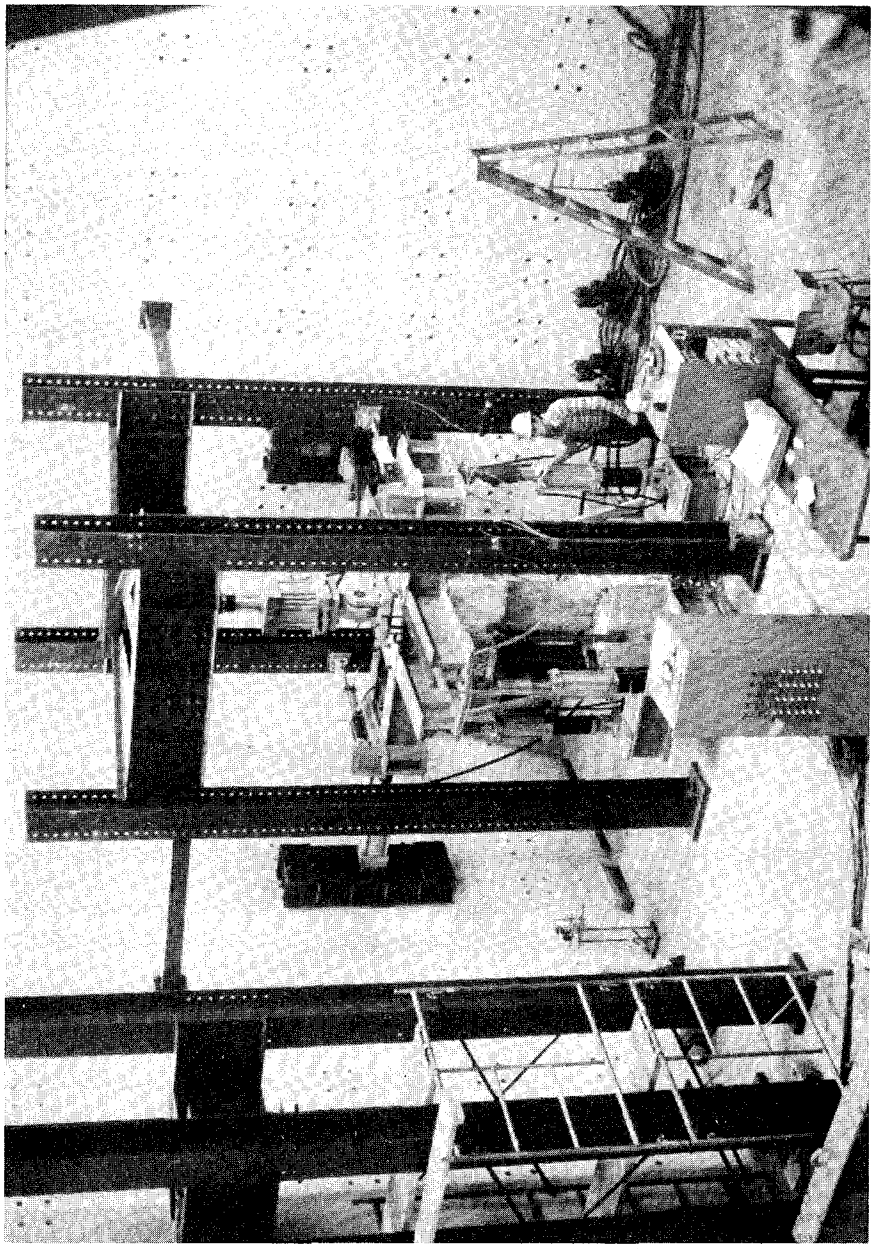

Fig. 3.6 Test setup

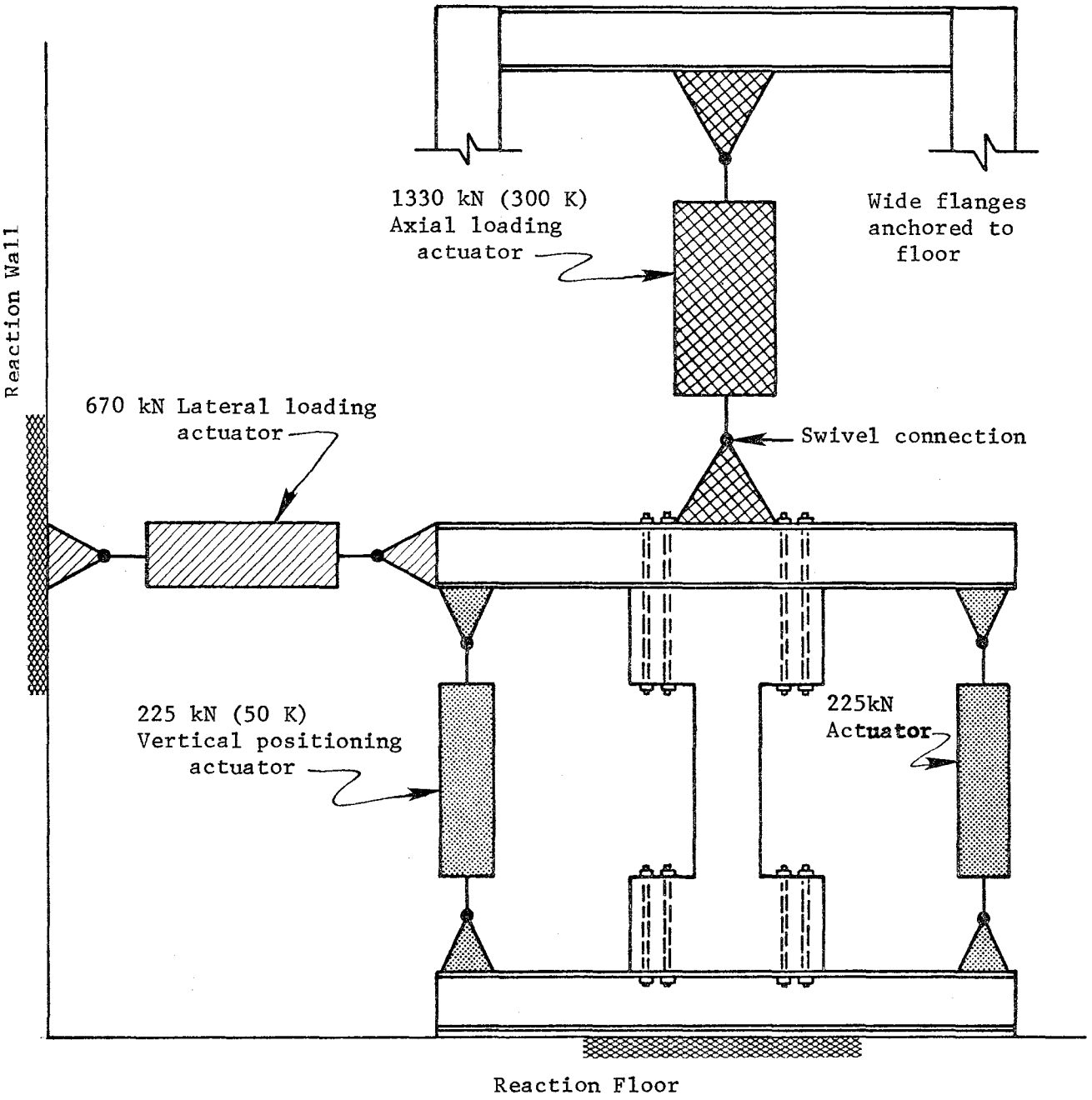

Fig. 3.7 Elevation of loading frame

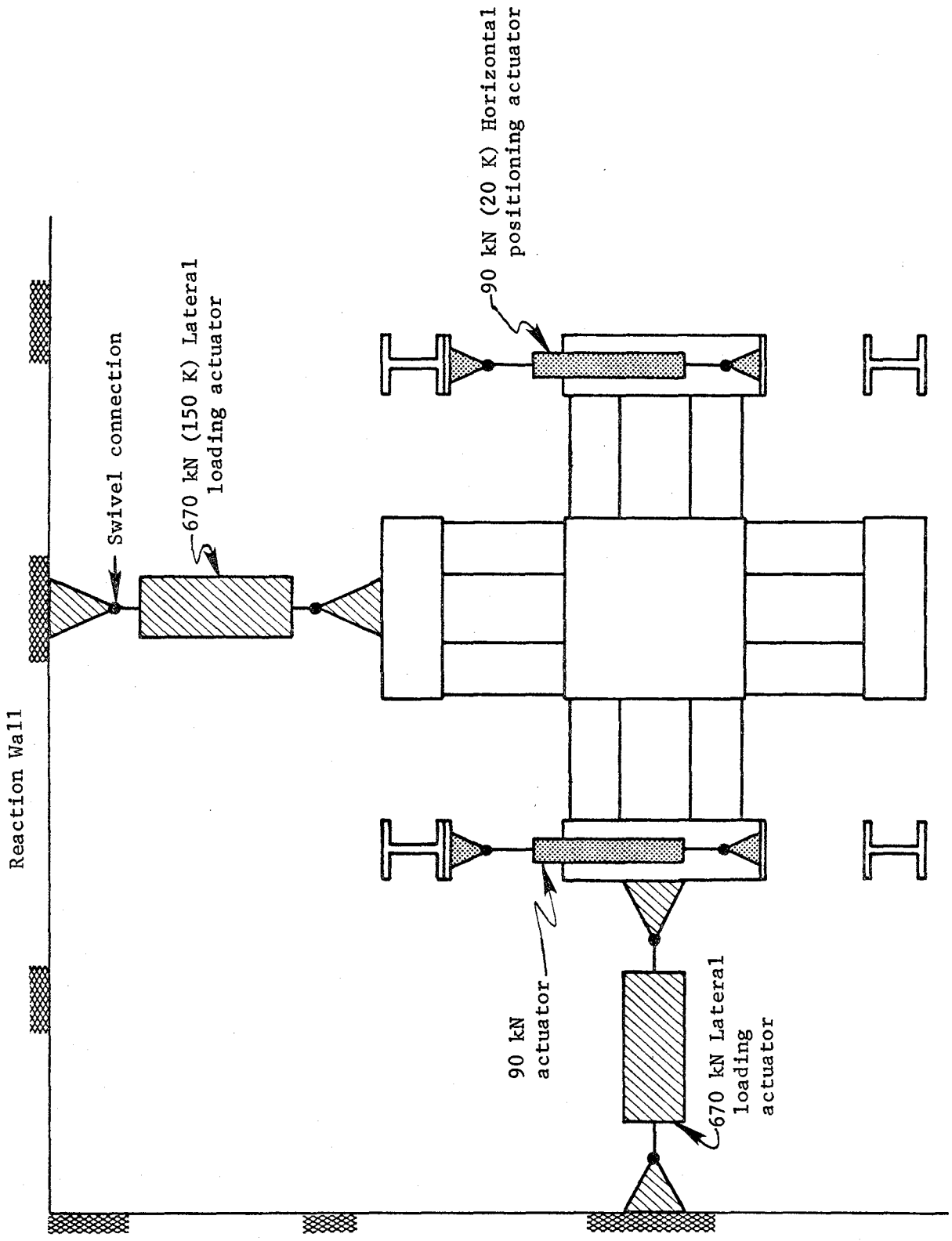

Fig. 3.8 Plan of loading frame

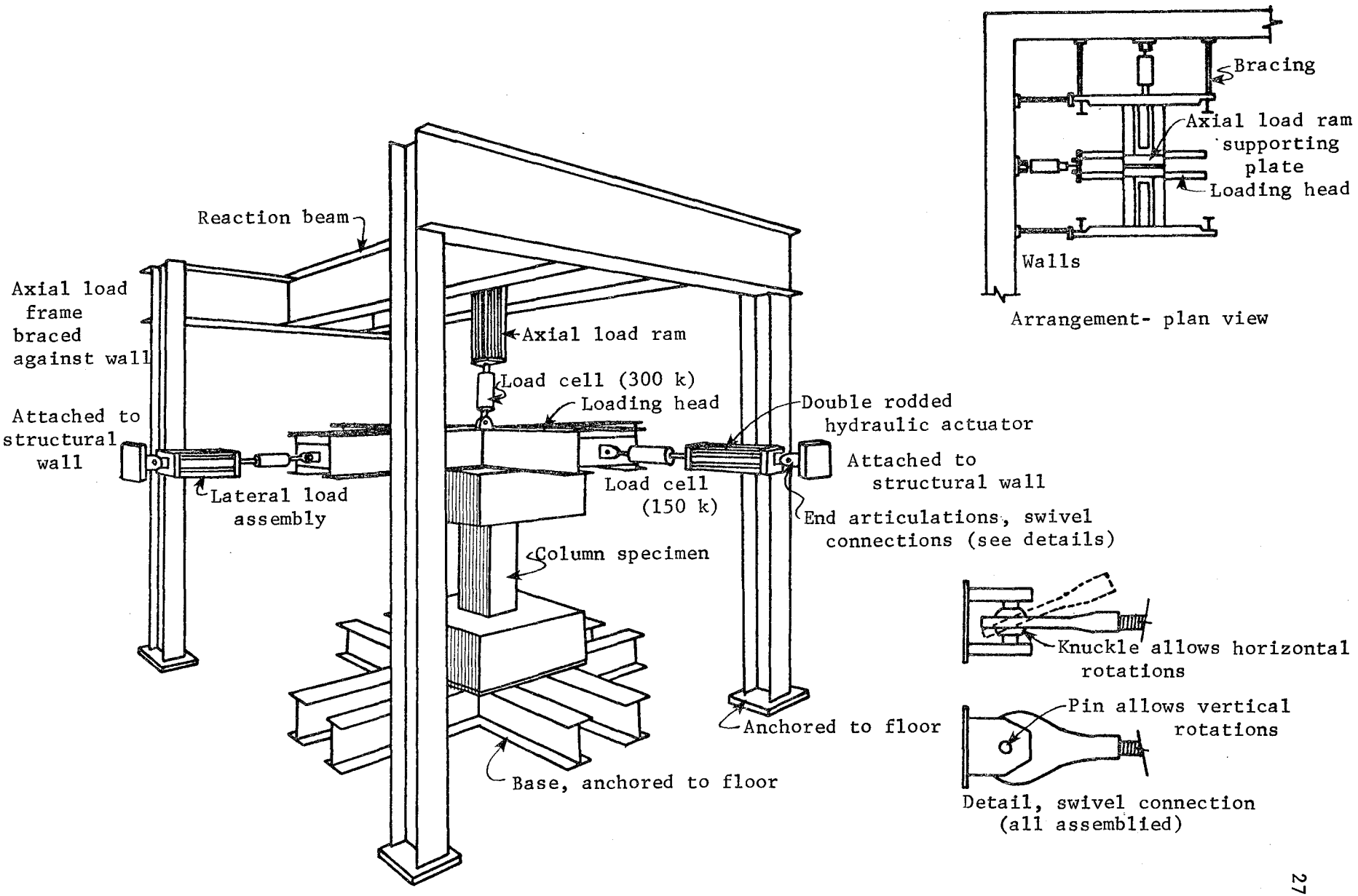

Fig. 3.9 Loading frame

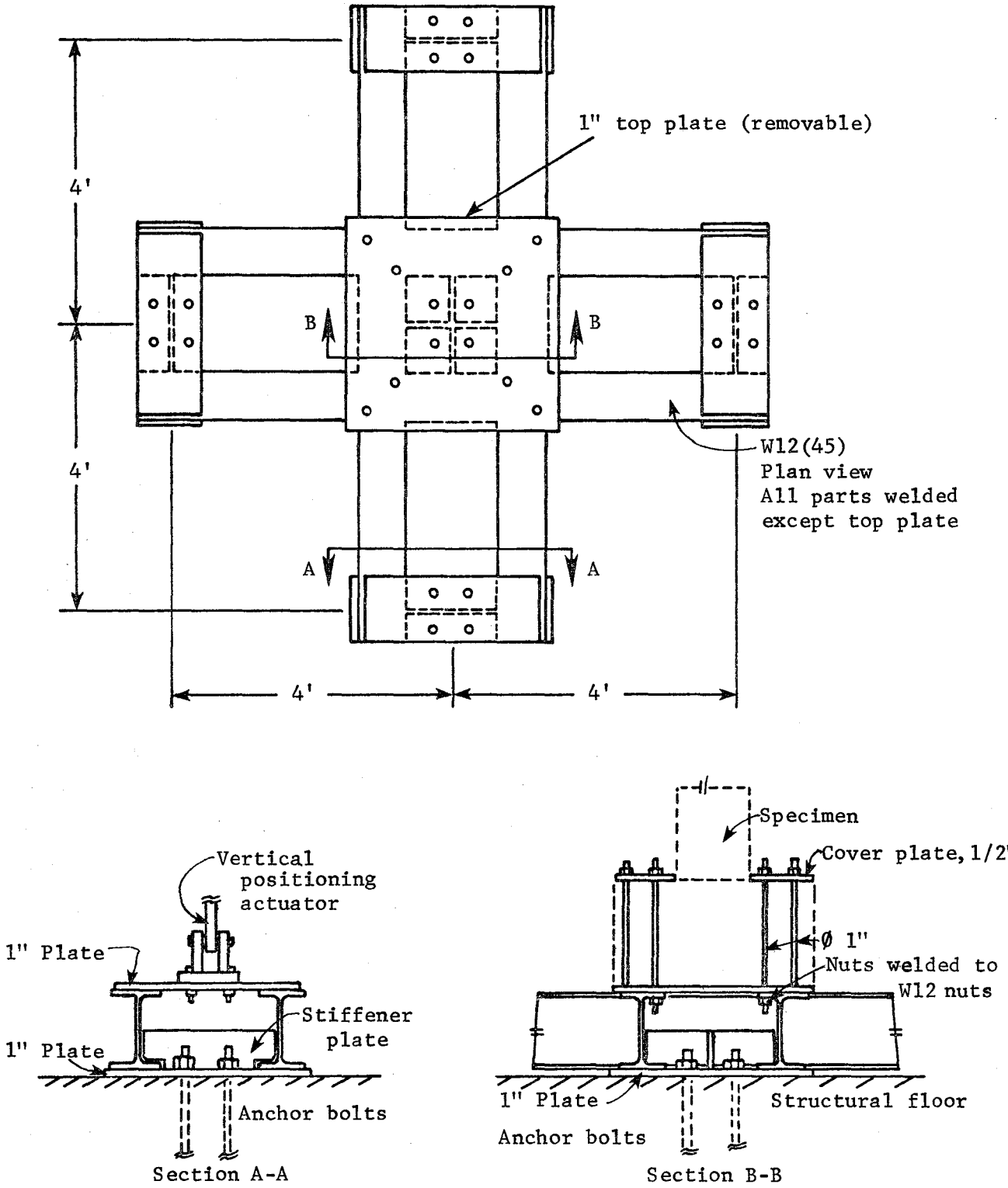

Fig. 3.10 Loading base details

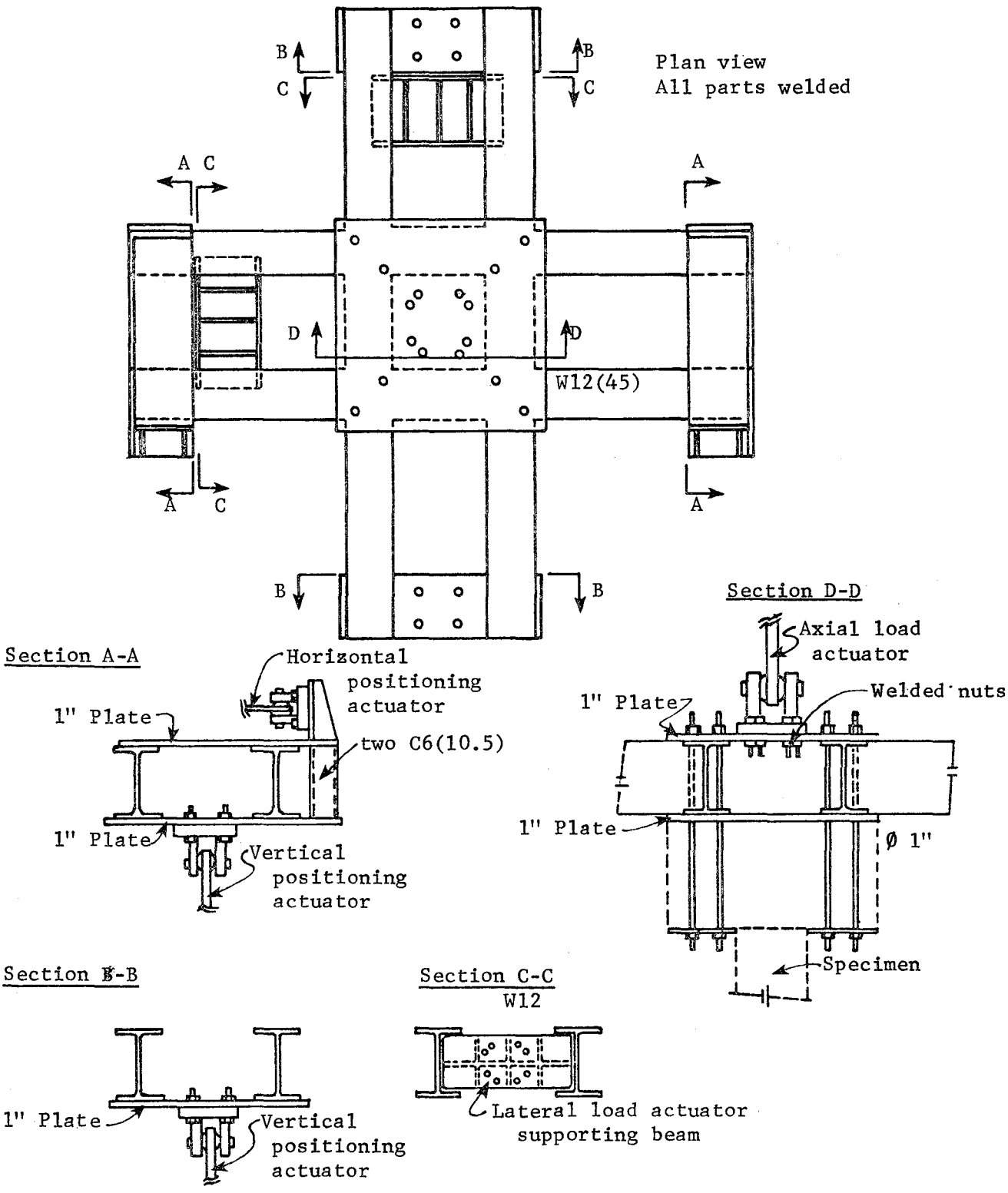

Fig. 3.11 Loading head details

axial load actuator is supported over the center of the setup with transfer beams made up of wide flanges bolted to the columns. The details of the frame as shown in Fig. 3.12. The transfer beams can be raised or lowered to accommodate changes in test column length. The axial load frame is braced against the walls of the floor-wall reaction system for stability.

3.6 Hydraulic Position System

The function of the hydraulic positioning system has been described previously. The system is shown in detail in Fig. 3.13. The system is based on using pairs of cross-coupled, double-rodded actuators to resist rotation but not translation, as shown in Fig. 3.14. All positioning actuators have swivel heads at each end which permit articulation in any direction. The swivel heads were purchased with a "zero-backlash" feature to improve the performance of the positioning system. In each pair of actuators one load cell is used to provide a direct measurement of the force required to resist rotation. The vertical positioning actuators have an effective area of about 19 $in.^2$ and a 12 in. stroke. The horizontal actuators have an effective area of about 6 $in.^2$ and a 12 in. stroke.

The actuators are cross-coupled with high pressure hydraulic hoses. Shut-off valves and couplers provide flexibility to permit the actuators to be used for raising or lowering the head or adjusting the initial position of the head prior to placement of the test specimen. The hydraulic lines are initially pressurized to a level of about 2000 psi. This allows the system to operate on pressure changes which will not produce a vacuum in the lines. In addition, the initial pressure tends to stiffen the hydraulic hoses and reduces the flexibility of the positioning system.

In the early stages of operation, modifications in the internal seals of the actuators were required to eliminate leakage of oil past the seals. It should be noted that under usual operation the actuators are servo-controlled and oil bypassing the seals poses no problem. However,

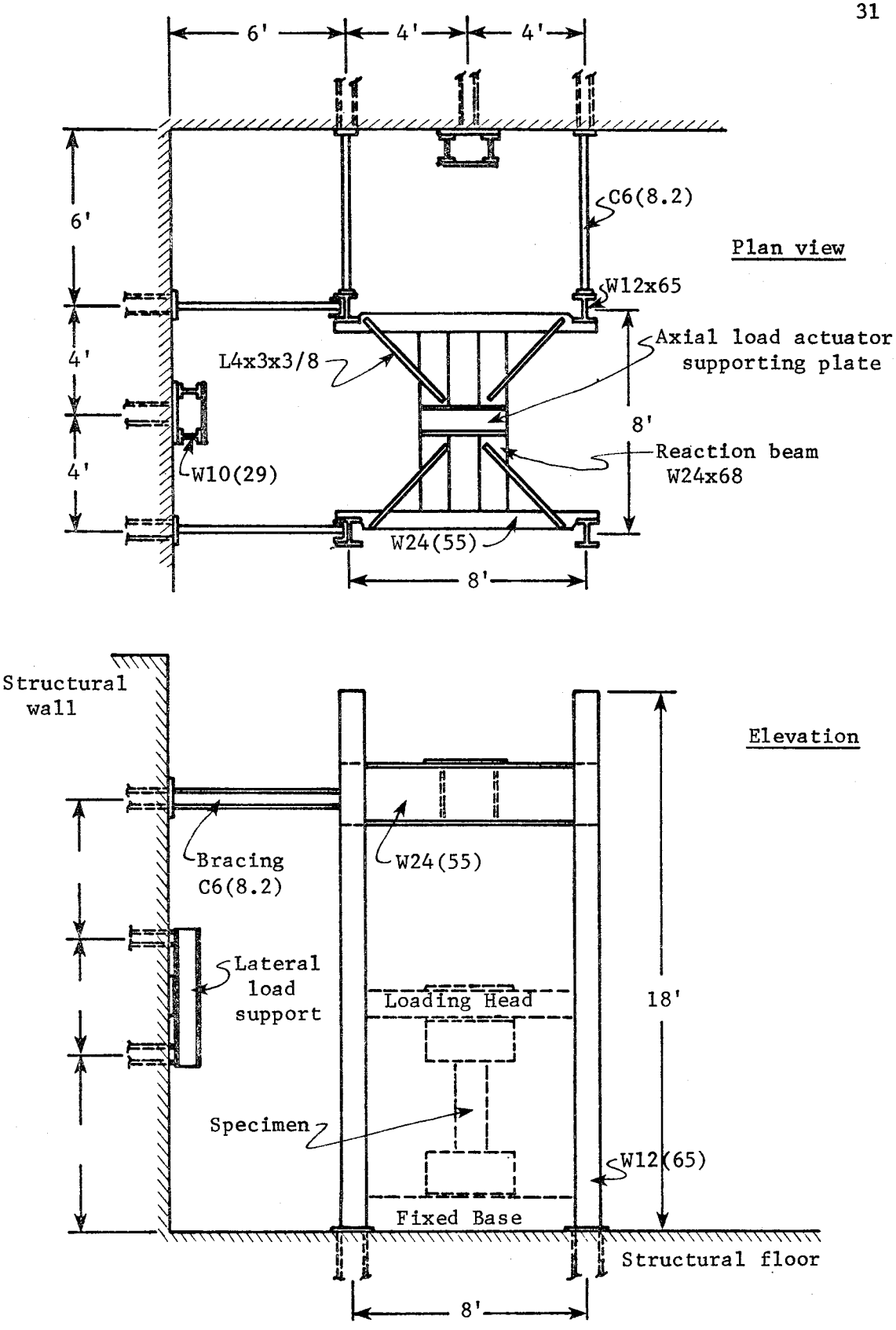

Fig. 3.12 Axial load frame

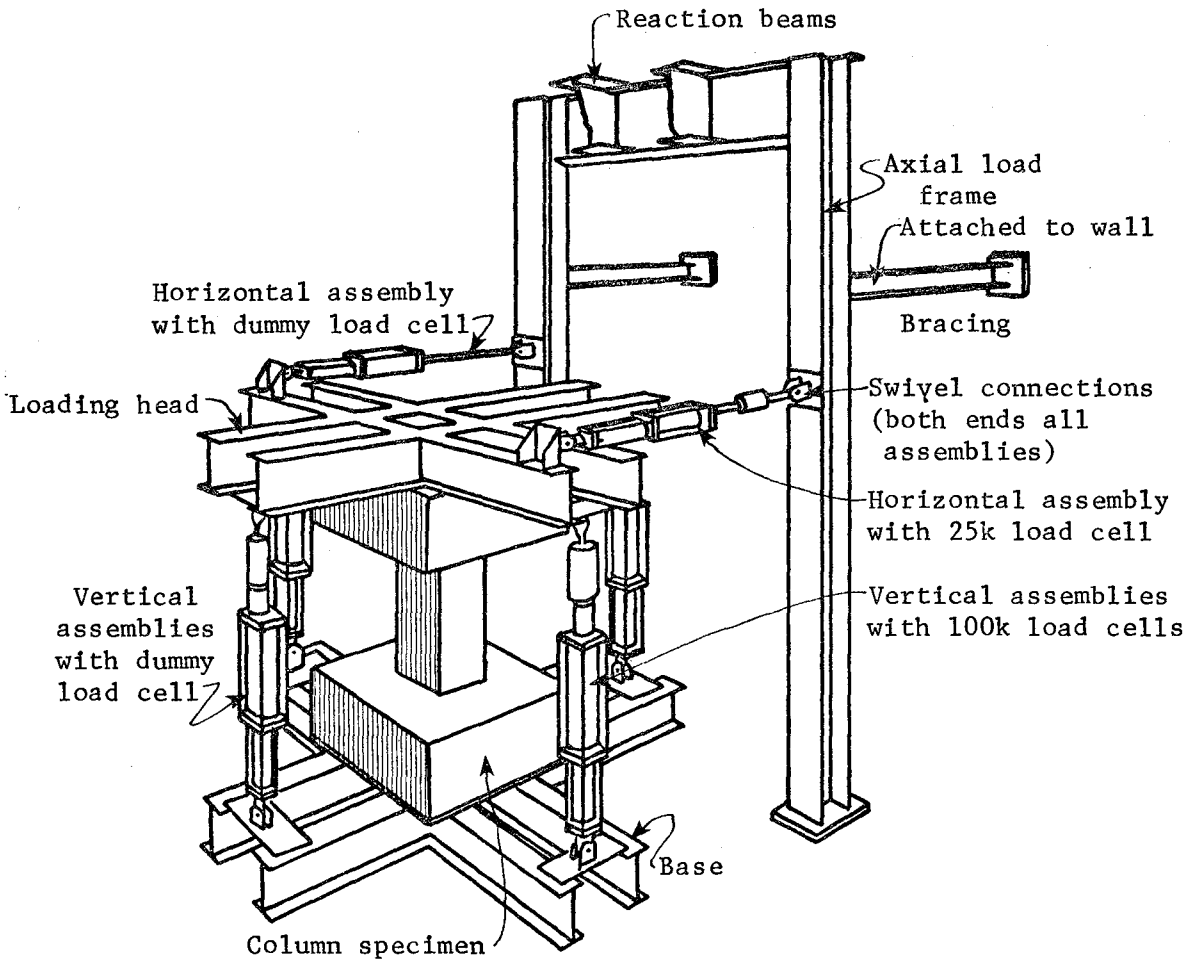

Positioning System - Schematic

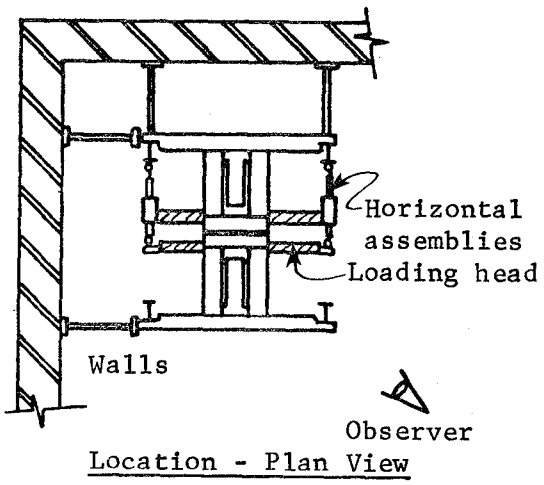

Location - Plan View

Fig. 3.13 Loading frame

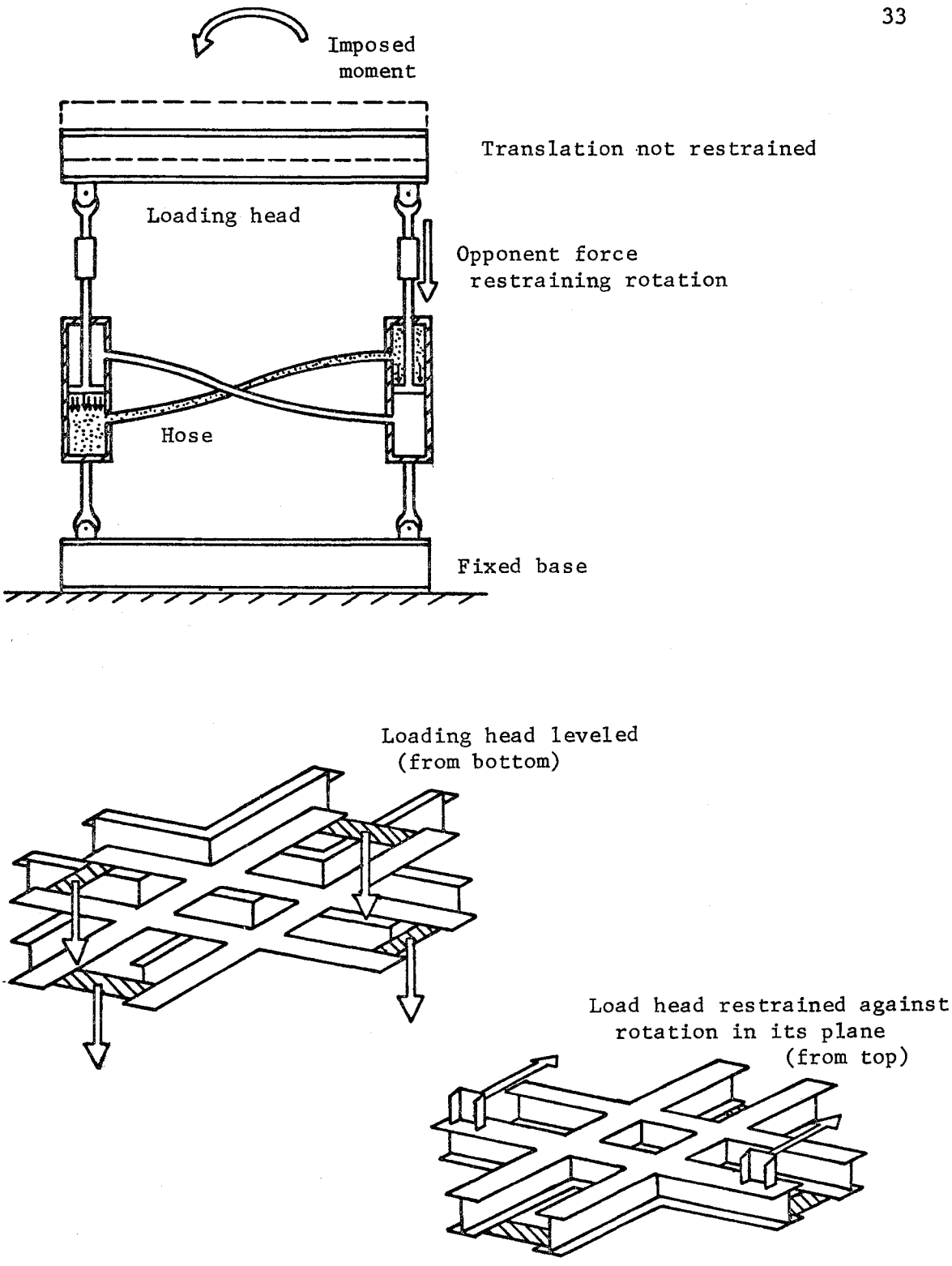

Fig. 3.14 Restraining function of paired hydraulic positioning actuators

controlled through the mini-computer with commands from a teletype console located on the floor next to the test area. In the manual mode, the deformation output from the specimen is monitored on an x-y recorder and the variable gain on the servo-control console adjusted until a desired level of deformation is reached.

CHAPTER 4

INSTRUMENTATION

4.1 Loads

Load cells were used to monitor applied loads and positioning forces. A 1330 kN (300k) load cell was used to measure the axial load. Two 670 kN (150k) load cells were used for lateral loading. Similar 450 kN (100k) load cells were used for the vertical positioning actuators in each direction. A 90 kN (25k) load cell was attached to one of the paired horizontal positioning actuators. The general arrangement of these load cells can be seen in Figs. 3.9 and 3.13.

All load data were recorded using the data acquisition system and were stored on magnetic tape. Selected loads were monitored on x-y plotters for visual observation during testing.

4.2 Displacements

As shown in Fig. 4.1, twelve ±1.0 in. LVDTs (linear variable differential transducers) were used for measuring lateral translations of the top end block and vertical displacements of top and bottom end blocks. The transducers were supported by the special frames. Two different frame supports were tried before a satisfactory system was devised. First, the stand shown in Fig. 4.2a was used for supporting the transducers. It was desired to measure the horizontal deformations of the top end block relative to the bottom and the rotations of the top column end block relative to the bottom block. The system gives the relative rotation of the column end block even though there may be rotation of the bottom end block. In the initial tests, the rotation of the bottom end block was considered to be negligible. The first six tests were conducted with this measuring system. During the sixth test in which loads were

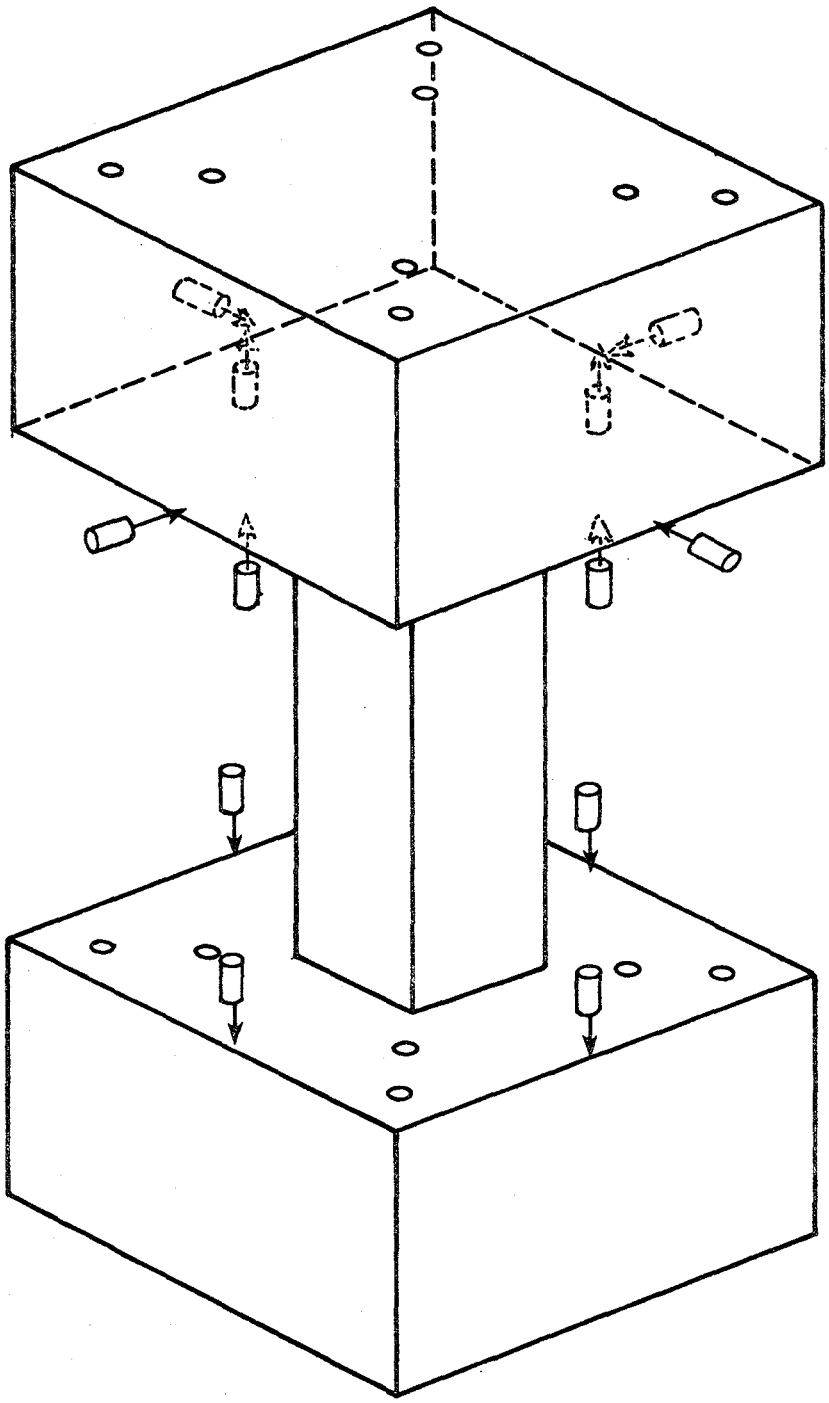

Fig. 4.1 Location of transducers

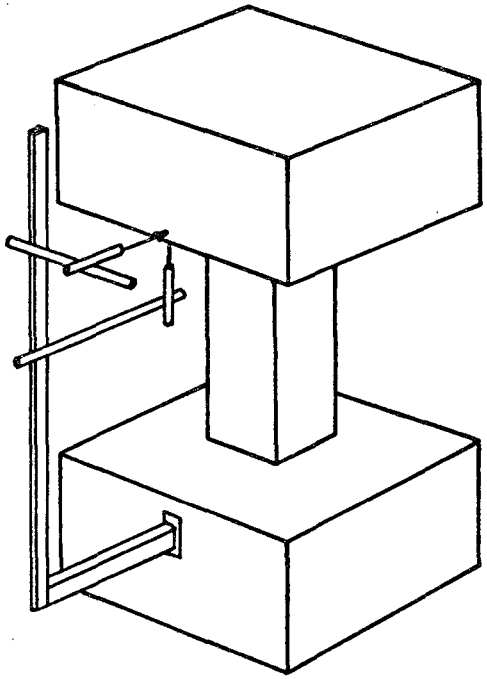

(a) Frame mounted on specimen

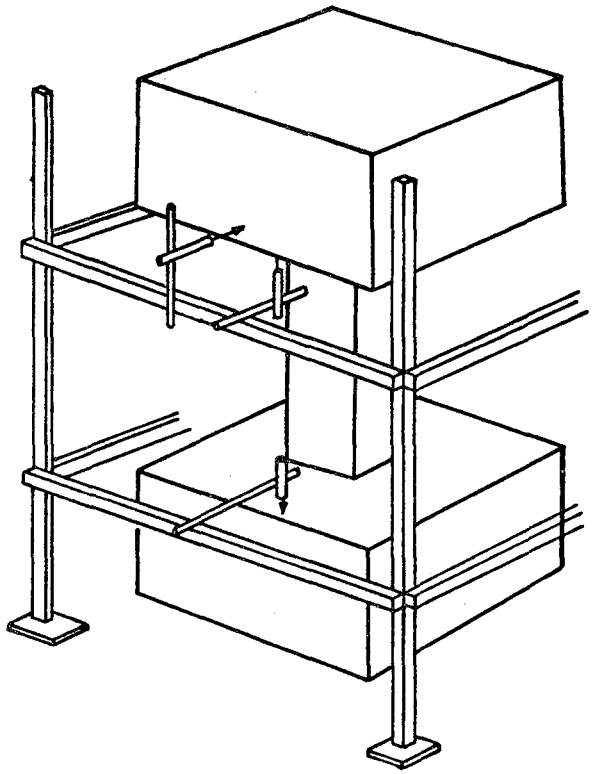

(b) Independent frame

Fig. 4.2 Deformation measurement

applied consecutively, rotations of the bottom end block produced effects which were not negligible. Because the bottom end block was not totally fixed, the bracket holding the transducer rotated and the relative deformation measured was less than that applied. The real deformation was 10 $\sim$ 20 percent higher than the measured value.

After it was realized that the influence of the rotation of the bottom end block was not negligible, a different system, shown in Fig. 4.2b, was developed. The measuring frame which supports transducers was isolated from the test specimen and the loading frame. Four transducers were added in order to measure the rotation of the bottom end block. The translation of the bottom end block was not measured because earlier tests indicated it was less than 2 percent of the lateral deformation of the column and could be neglected. All subsequent tests have been conducted using the independent support frame for the transducers. Based on the measured rotation of the bottom end block, the rotations of the bottom end block in the initial tests were estimated and the lateral deformations adjusted.

Deformations were monitored by the data acquisition system and on x-y plotters for obtaining load-deflection curves during testing. Mechanical dial gages were used in a few tests to measure the twist of the column head and the efficiency of the horizontal positioning system. Once this was shown to be working well, further measurements were deemed unnecessary.

4.3 Strains

Strains in transverse and longitudinal reinforcement were measured throughout the test. As shown in Fig. 2.1, strain gages were attached on all four legs of every other tie along the height of the column and on two diagonally opposite longitudinal bars at the critical end sections. Wire resistance strain gages (0.64 in. long) were attached prior to casting and waterproofed. Leads extended to the outside of the forms. Strains were recorded using the data acquisition system.

4.4 Data Recording and Processing

The data acquisition system is based on a VIDAR scanner with a multi-mode recording capability. A block diagram of the system is shown in Fig. 4.3. Data are initially recorded on magnetic tape or the disc unit. Following completion of the test, data are processed on the mini-computer and line printer tabulations are obtained of basic information by load stage. The processed data arrays can then be operated on to produce plots on the digital unit which can be processed in report quality format. With the system, large volumes of data can be processed quickly and evaluated before subsequent tests are conducted.

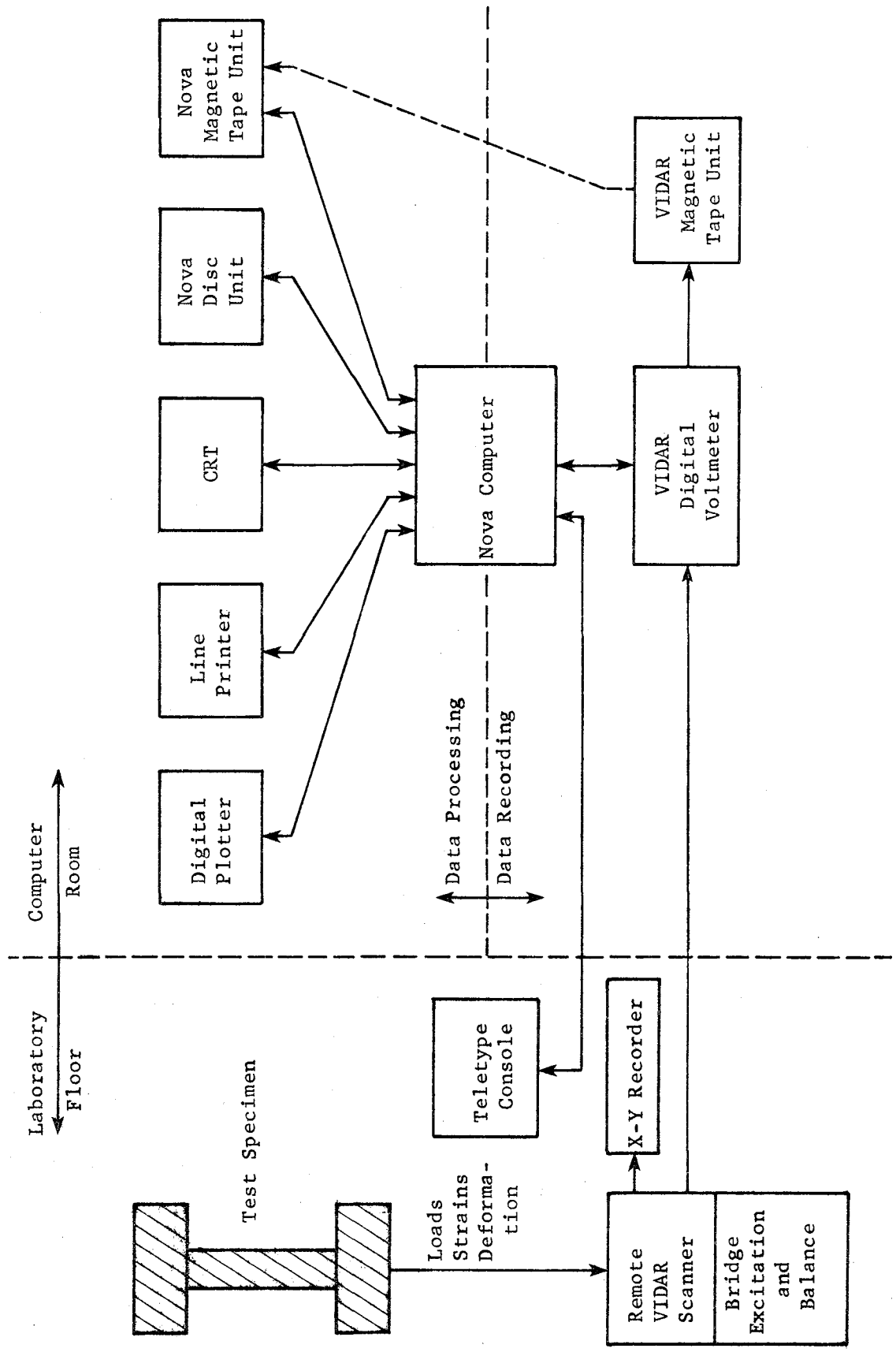

Fig. 4.3 Data recording and processing system

CHAPTER 5

INITIAL TESTS

5.1 Introduction

To demonstrate the capabilities of the loading and instrumentation systems developed, the results from four tests from the initial test program will be discussed. It is important to note that the basic geometry of the specimen and the reinforcement were identical for all tests, only the loading histories were changed. Axial load was zero throughout the tests. There were some differences in material properties between specimens. For each of the four tests, the loading history is described and the lateral load-deflection curves are presented for the principal axes of the specimen. The distribution of strains in the transverse reinforcement is discussed briefly.

For purposes of comparison, the load-deformation relationship for a specimen loaded monotonically to failure is plotted and designated with the symbol M. The results obtained give an indication of the influence of various load histories on the performance of the short columns in shear. A program of testing is in progress in which other loading histories are being studied. Variations in the axial load on the column (tension and compression) are included.

5.2 Loading History U

Figure 5.1 shows the basic unidirectional loading history U. The pattern consisted of three cycles at each deformation level with full reversal. The peak deformation in each three-cycle group was a multiple of the initial deflection Δ_i. The initial deflection was selected to correspond to the deflection at which the longitudinal column reinforcement exhibited yielding at the ends of the column. The selection of an

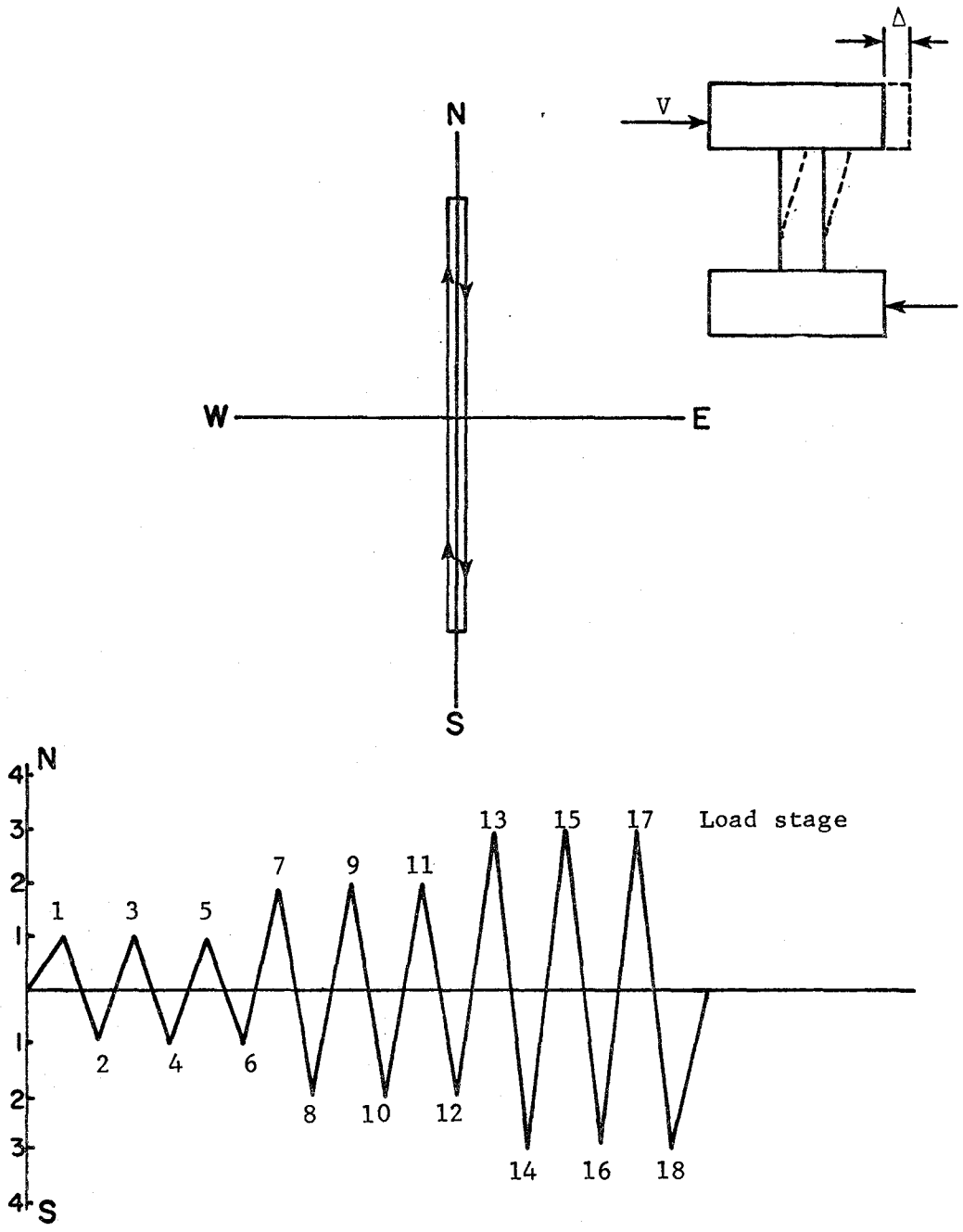

Fig. 5.1 Loading history U

initial deflection level is somewhat arbitrary because the specimens fail in a shear mode and elastic or yield deformations are difficult to calculate. The value of Δ_i is about 0.2 in. (5 mm). For ease in interpreting the load-deflection relationships, the peaks in the load history are numbered consecutively and are noted on the load-deflection curves.

Figure 5.2 shows the load-deflection curve for loading history U. It is apparent that the cyclic unidirectional reversals did not influence the shear capacity at higher deformation levels. Note that cycles 1, 7, and 13, and 2, 8, and 14 all reach the envelope curve for monotonic loading (M) to failure. With continued cycling at a given deformation level, there was some reduction in shear capacity, e.g., cycles 13, 15, and 17.

5.3 Loading History B

Figure 5.3 shows loading history B in which cyclic loads were applied alternatively in the principal directions (bidirectional loading). The same basic pattern is used with three cycles at each load level in each direction. Figures 5.4 and 5.5 show the load-deflection curves for the NS and EW axes. There is very little difference in the performance of the specimen in the two directions. Substantial decreases in capacity from the monotonic strength were observed at large deflection levels. There was also a gradual reduction in peak strength at each subsequent load stage at a given deflection level. Note the peak shear at load stages 13, 14, 19, 20, or 37, 38, 43, 44. Load was first applied in the NS and then the EW direction. As a result, the north peak lies very close to the monotonic curve (load stage 13), reduces slightly at load stage 14, and reduces further at peaks 19 and 20.

5.4 Loading History D

Figure 5.6 illustrates loading history D, in which the specimen was subjected to deformations along diagonals. Three cycles of load were applied along each diagonal at each deformation level. Figures 5.7 through 5.10 show the load deflection relationships for the principal

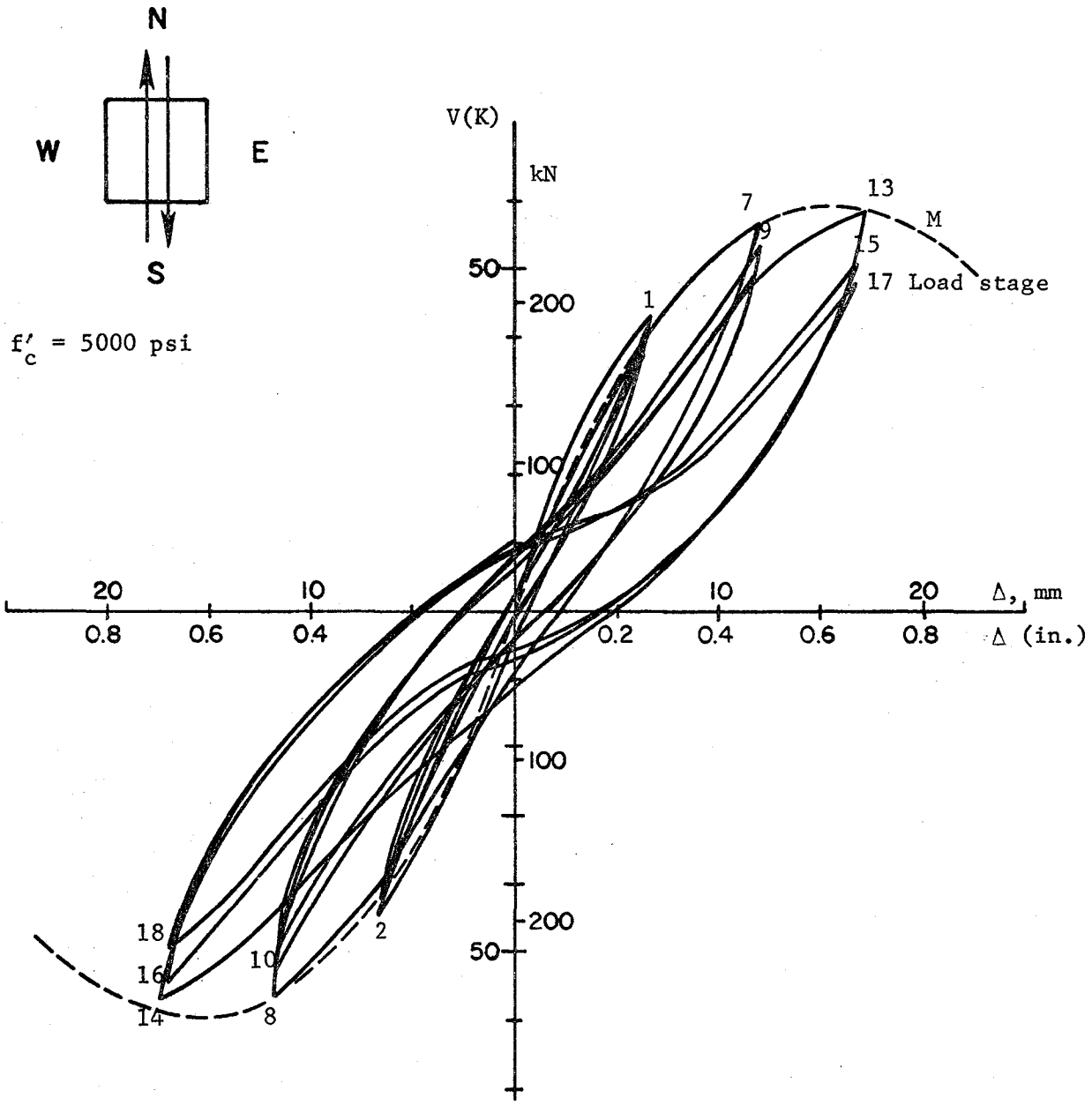

Fig. 5.2 Load-deflection relationship - U

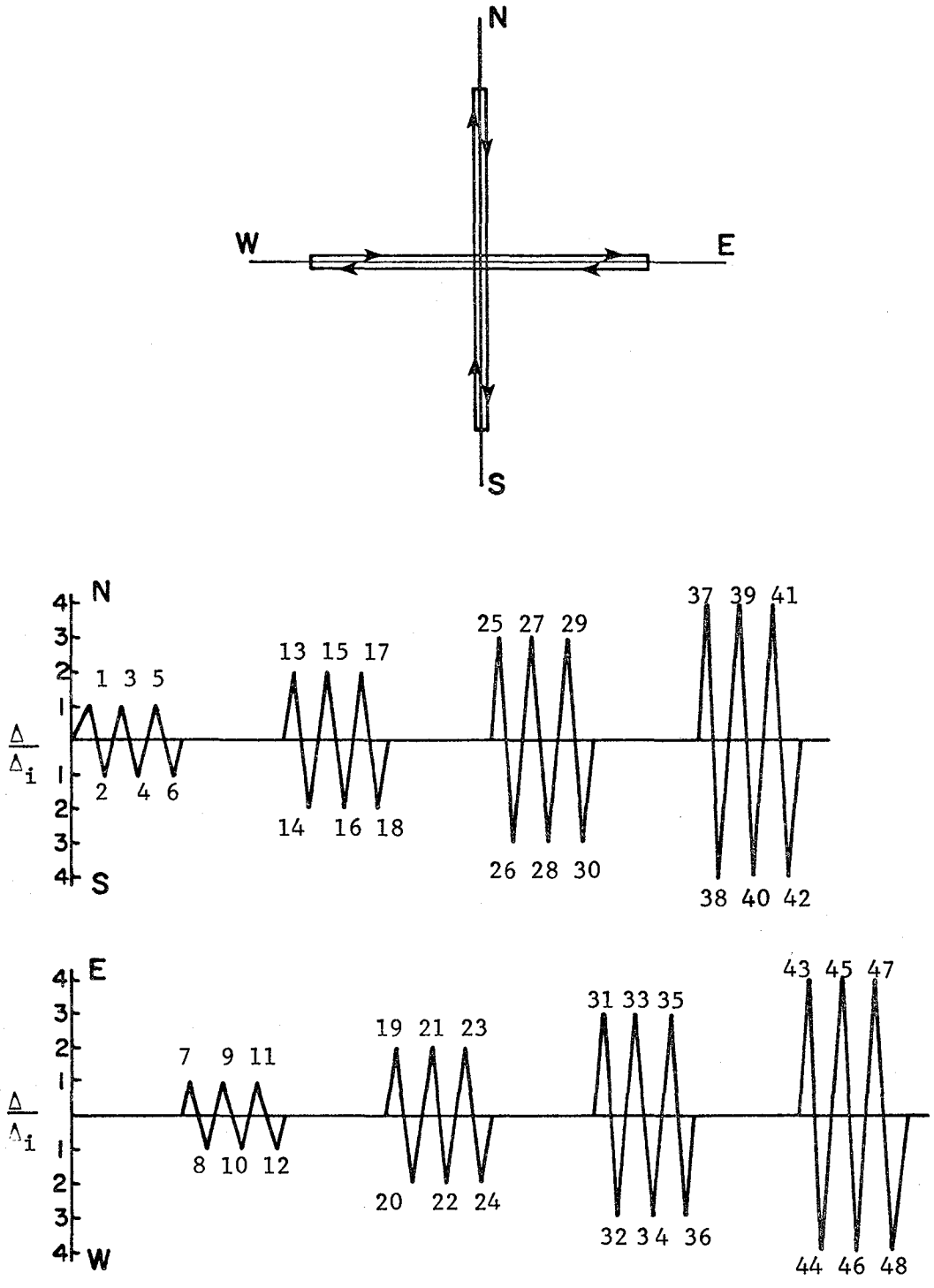

Fig. 5.3 Loading history B

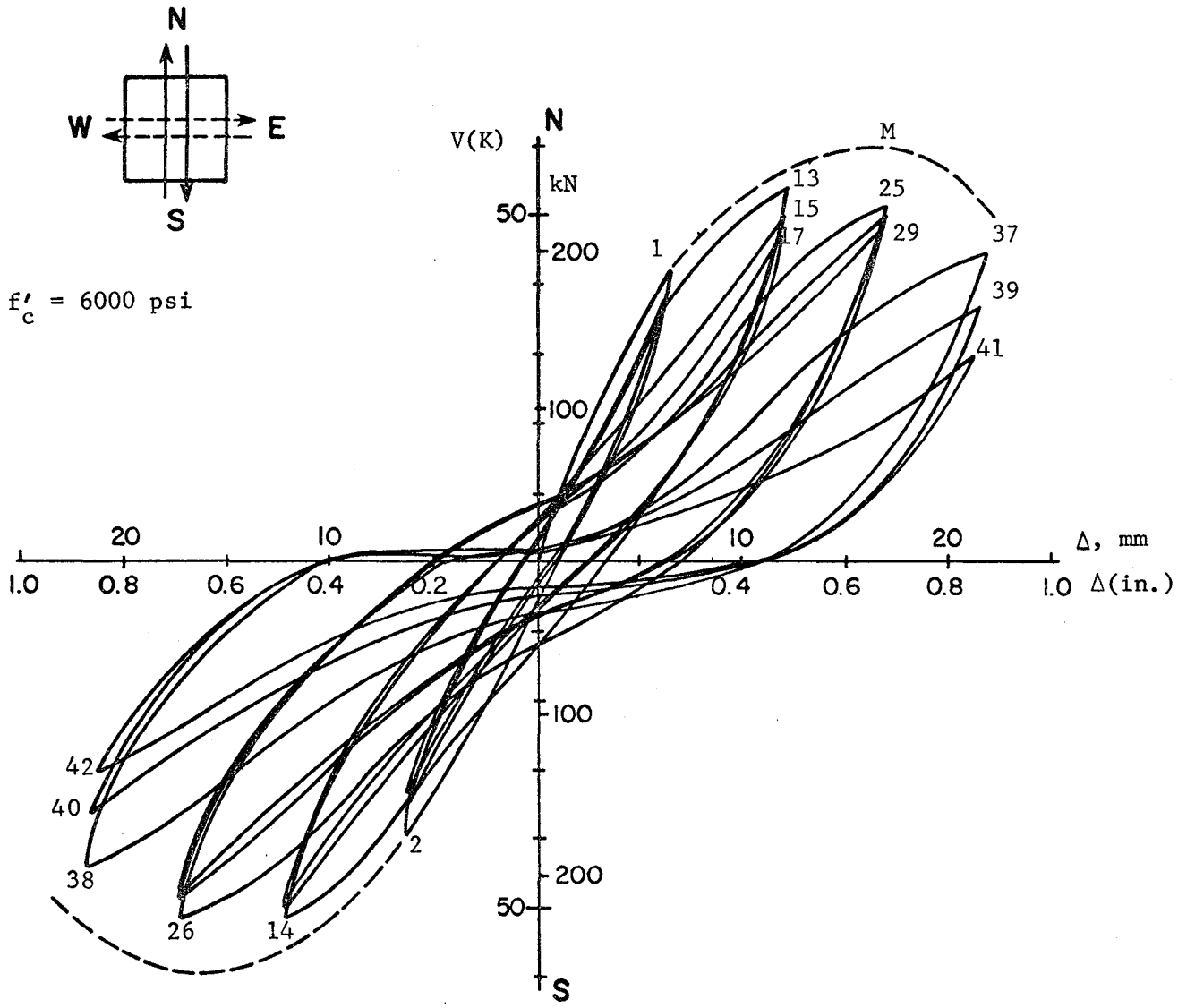

Fig. 5.4 Load-deflection relationship - B
(NS direction)

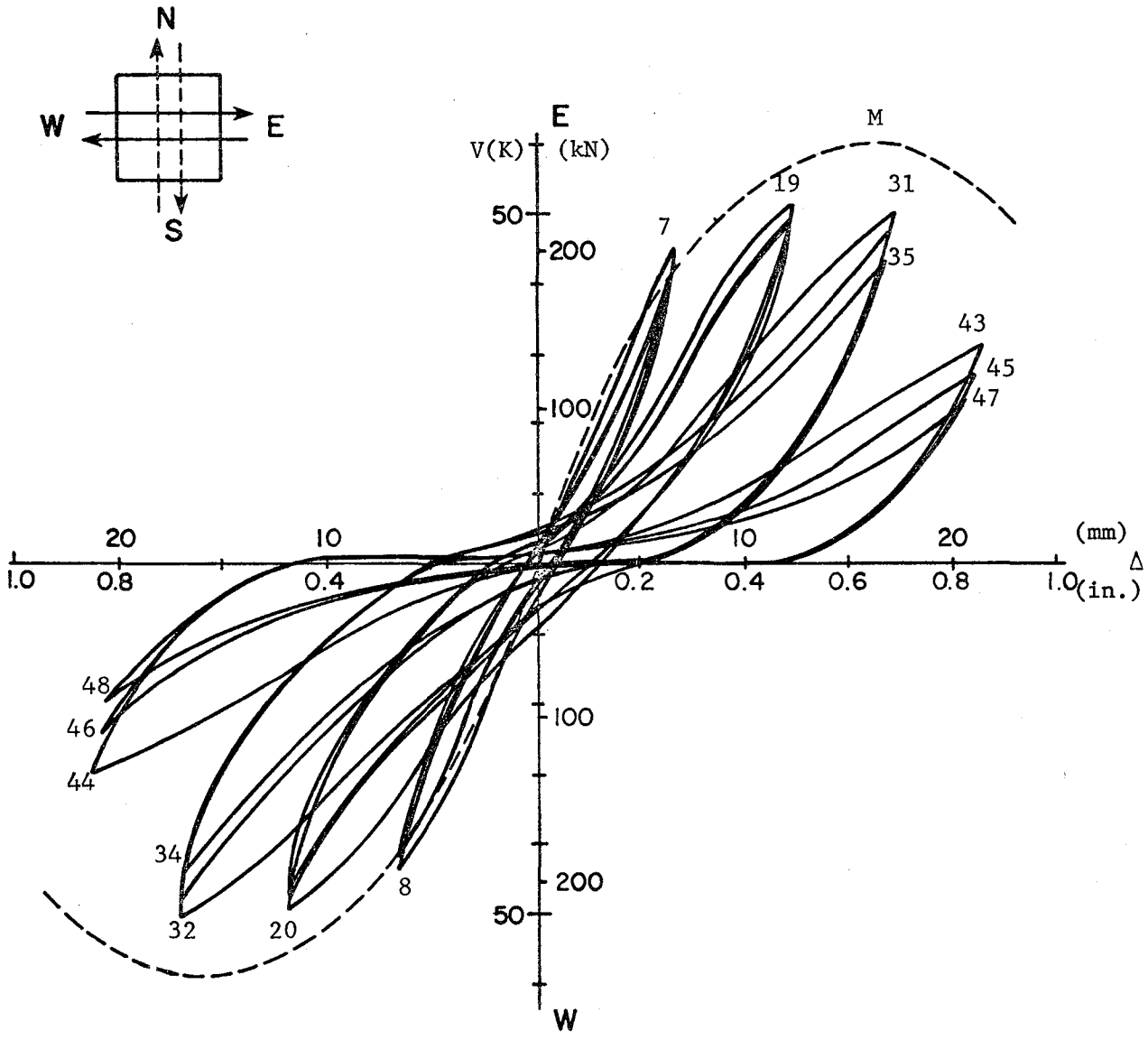

Fig. 5.5 Load-deflection relationship - B
(EW direction)

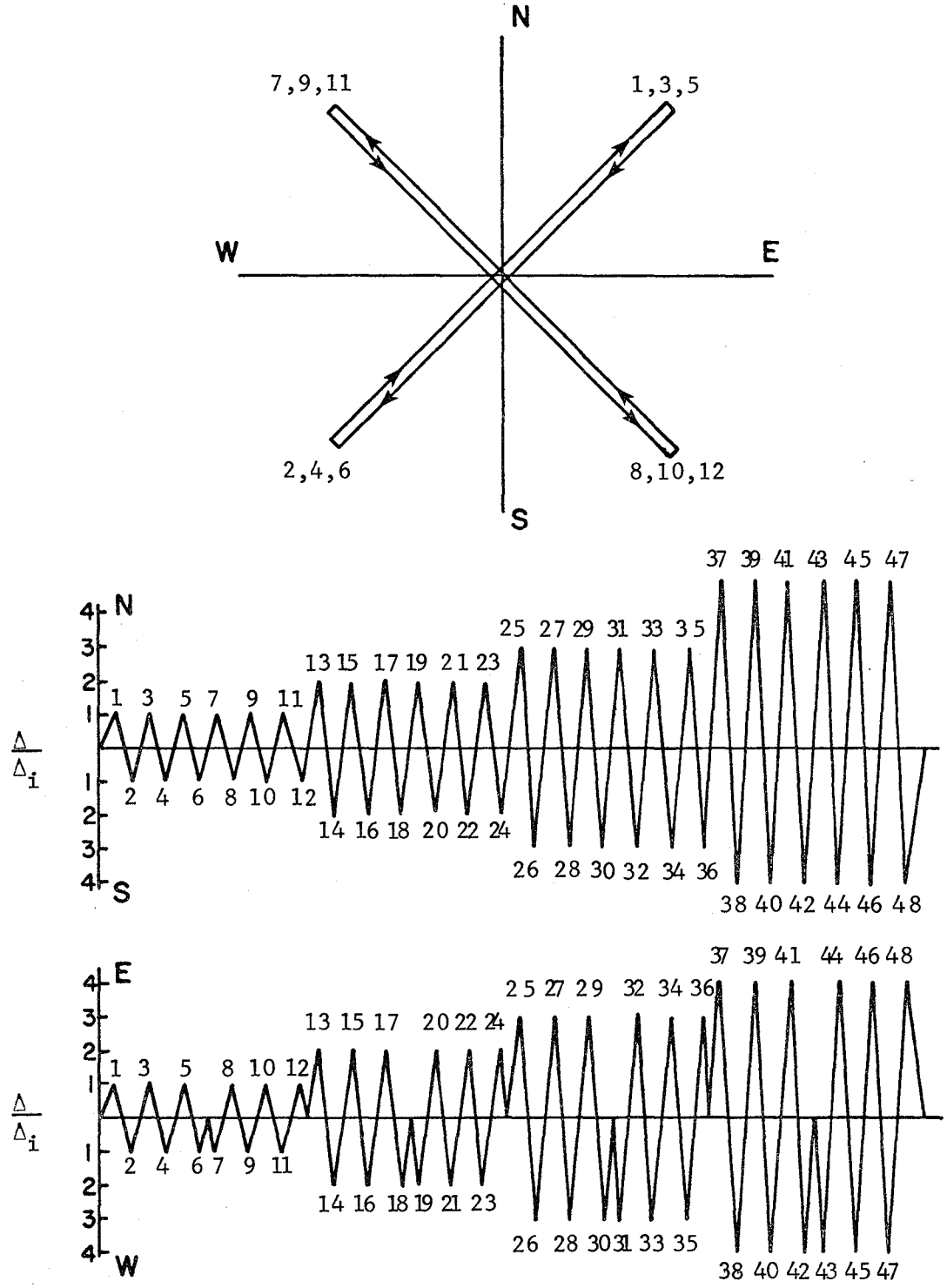

Fig. 5.6 Loading history D

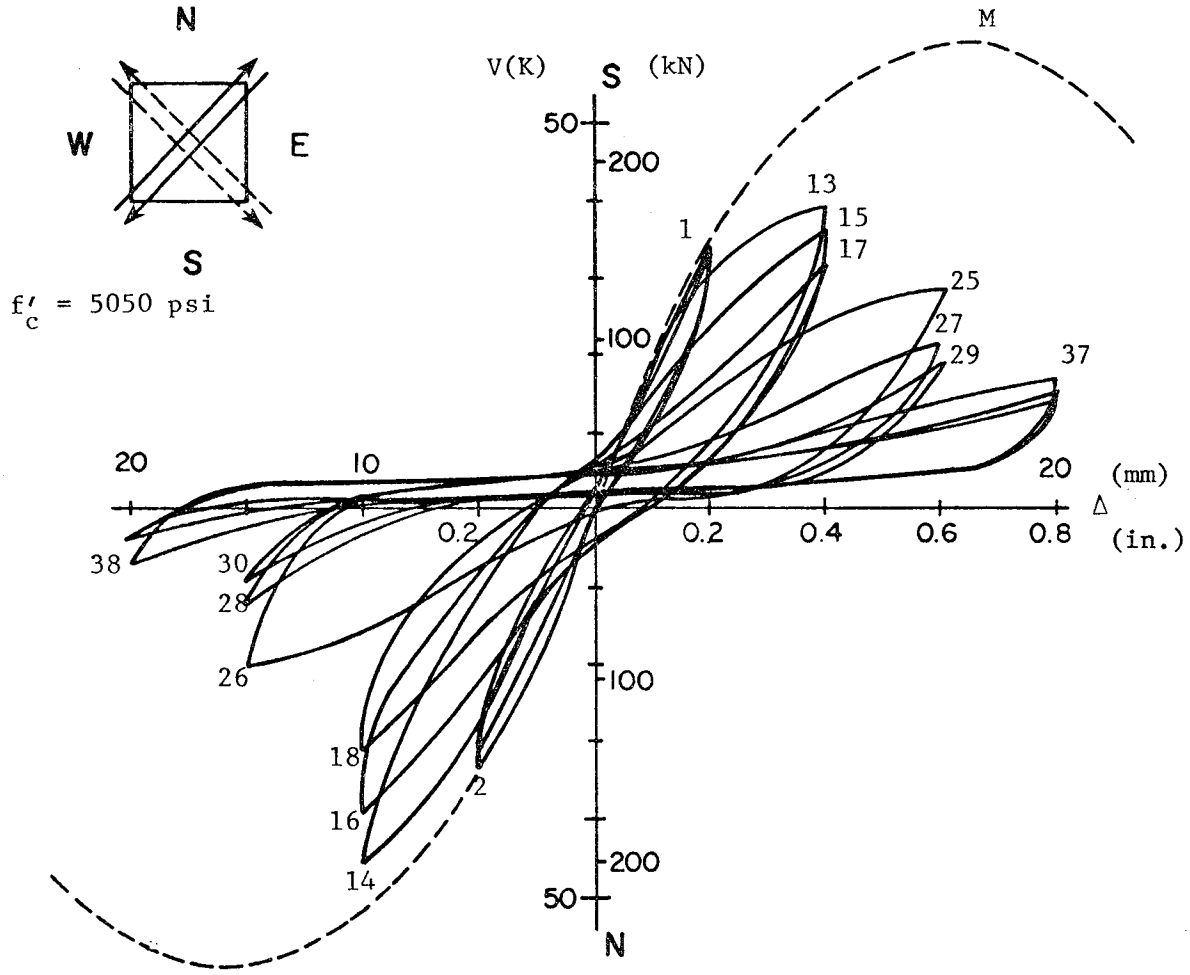

Fig. 5.7 Load-deflection relationship - D
(NS direction, NE-SW loading)

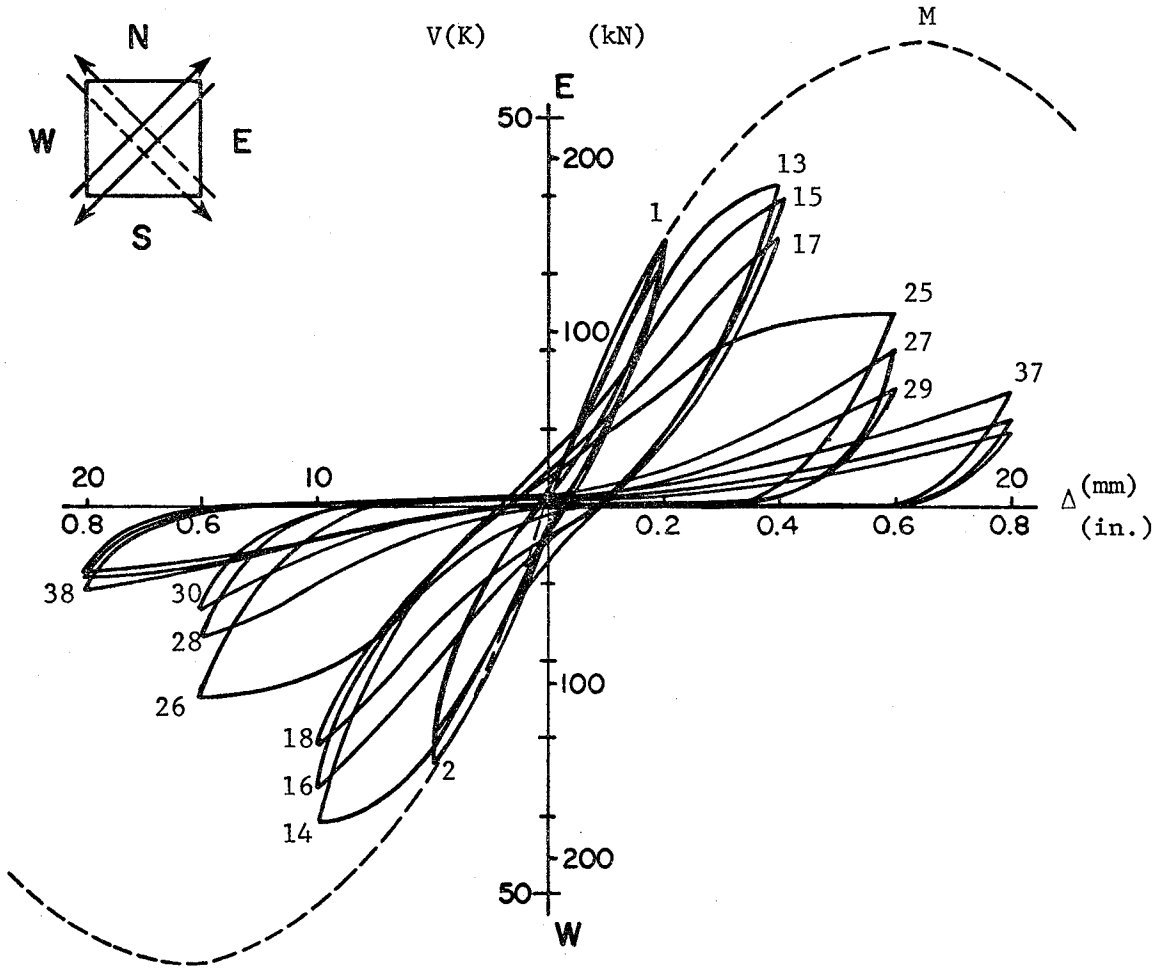

Fig. 5.8 Load-deflection relationship - D
(EW direction, NE-SW loading)

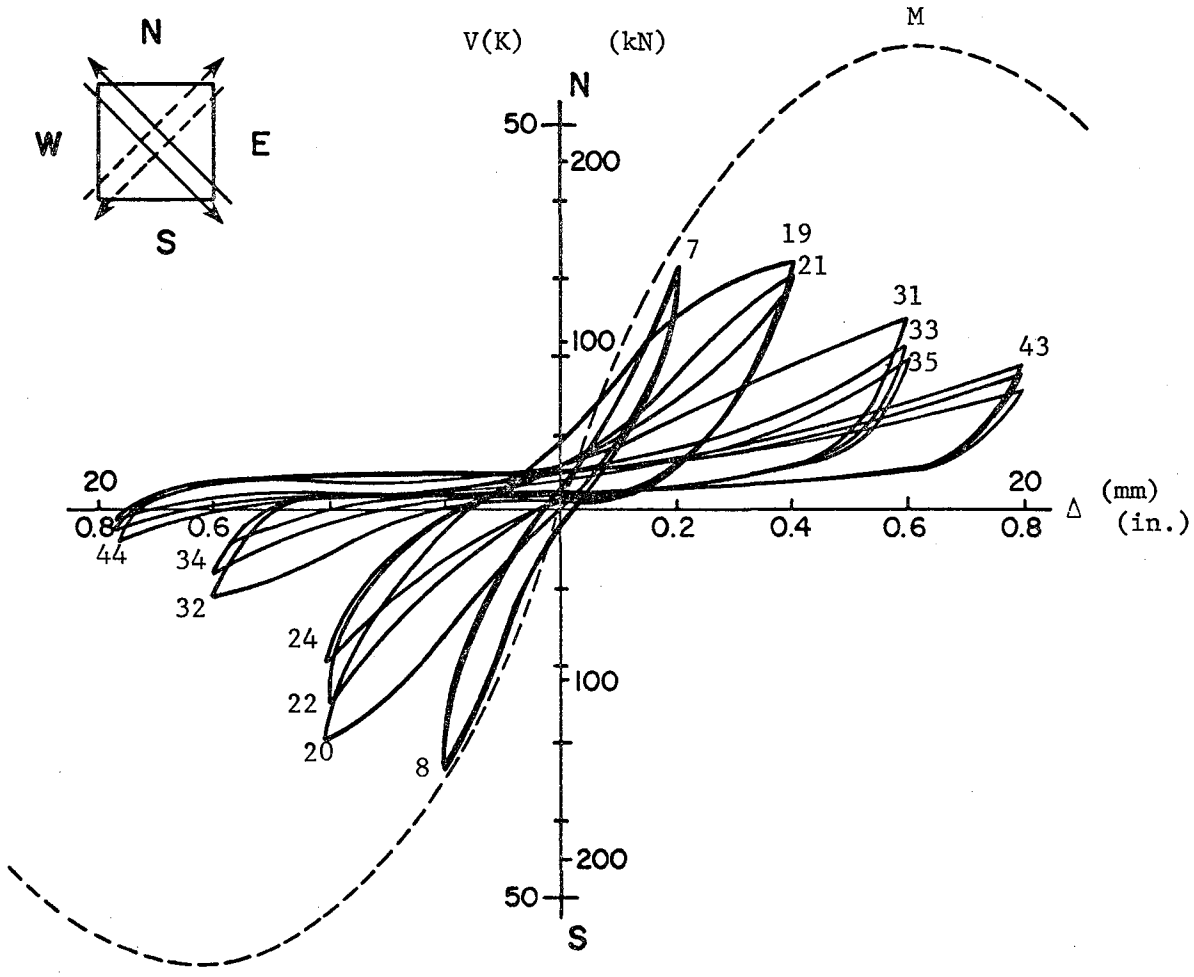

Fig. 5.9 Load-deflection relationship - D
(NS direction, NW-SE loading)

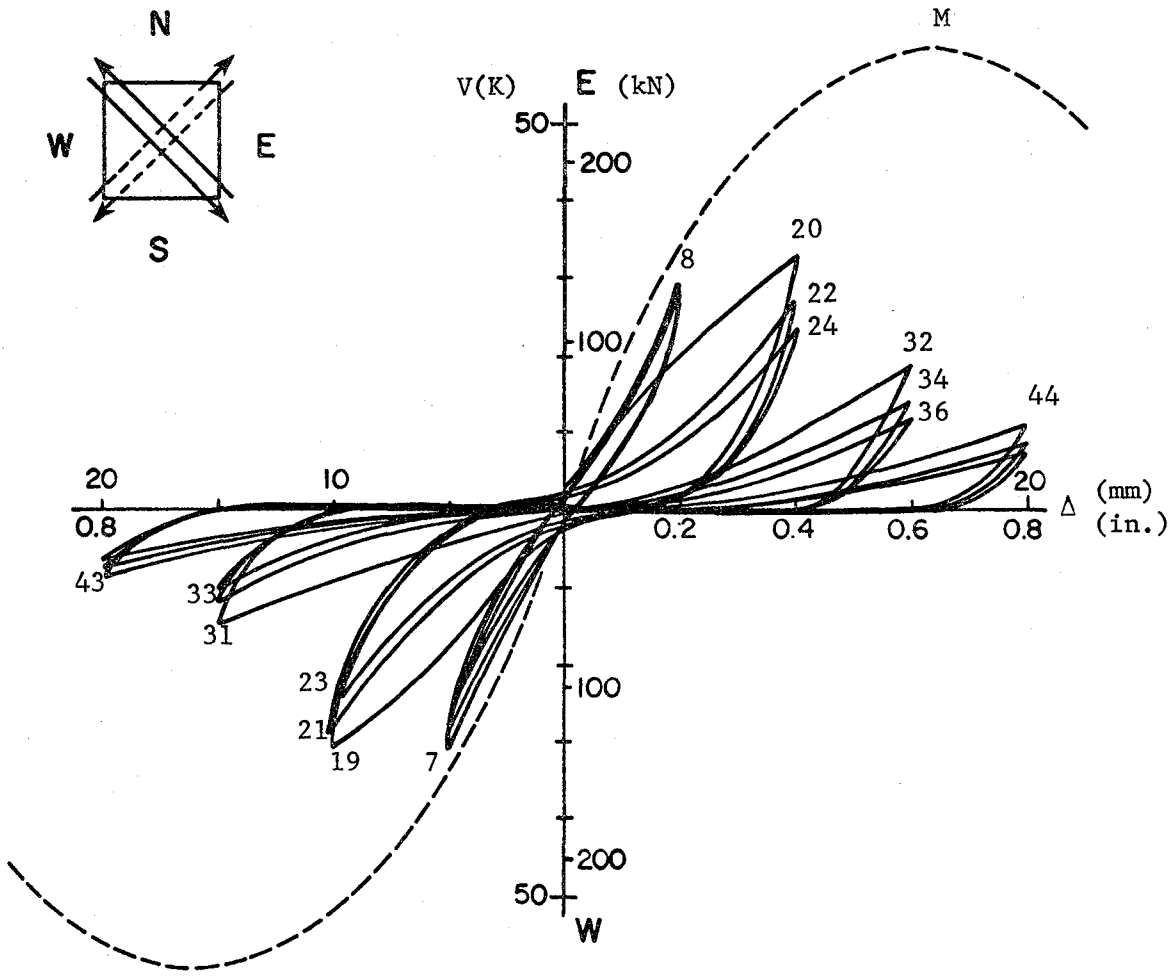

Fig. 5.10 Load-deflection relationship - D
(EW direction, NW-SE loading)

axes. For example, with loading along a NE-SW diagonal, shear components are developed along each axis and are plotted for the NS direction in Fig. 5.7 and the EW direction in Fig. 5.8. The load stages at the peaks coincide because under peak deflection in the NE loading, peak load is reached in both the north and east direction. Deflection levels were controlled along the principal axis so that the actual deformation path along the diagonal was longer than in U or B loading.

It is interesting to note that the response under the D loading shows large reductions in peak shear capacity and stiffness at all deformation levels beyond the initial deflection. First loading was always along thhe NE-SW diagonal and the strength was higher for NE-SW than for NW-SE loading. With the imposition of deformations in both directions to produce the diagonal pattern, it is obvious that very large reductions in shear capacity are produced and the reduction is most severe under large deformation levels.

5.5 Loading History S

Figure 5.11 illustrates loading history S. Under this loading the deformation path traced by the top end of the column with respect to the bottom is a square. Each square was repeated three times at a given deformation level. The deformation level was determined along the principal axis. With this pattern, the deformation at load stages 2, 15, 28, and 41 would be identical to that at load stages 1, 13, 25, and 37 in loading history D. The purpose of the test was to examine if the path of loading, as well as the deformation, was significant.

Figures 5.12 and 5.13 show the load-deflection curves for the NS and EW direction. Under the initial deflection level of 0.2 in. (5 mm), the curves are stable and nearly identical in both directions. However, on increasing the deflection level several phenomena are apparent. A rapid decrease is noted in the peak capacity at the "corners" of the square. For example, there is a large reduction in shear strength from load stages 14, to 18 to 22. Note also, the reduction in shear force under the deformation along a "side of the square". When load stage 17 is

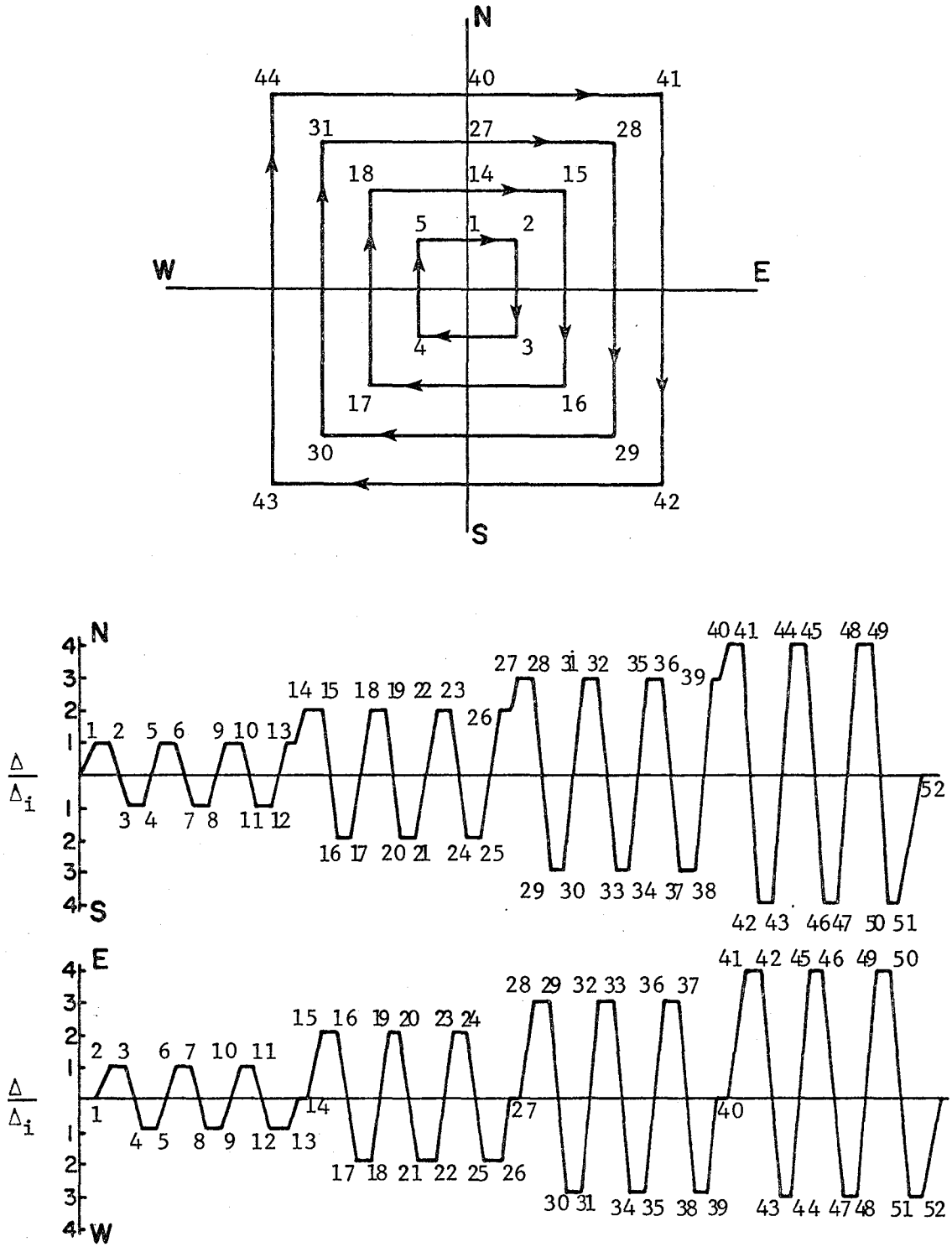

Fig. 5.11 Loading history S

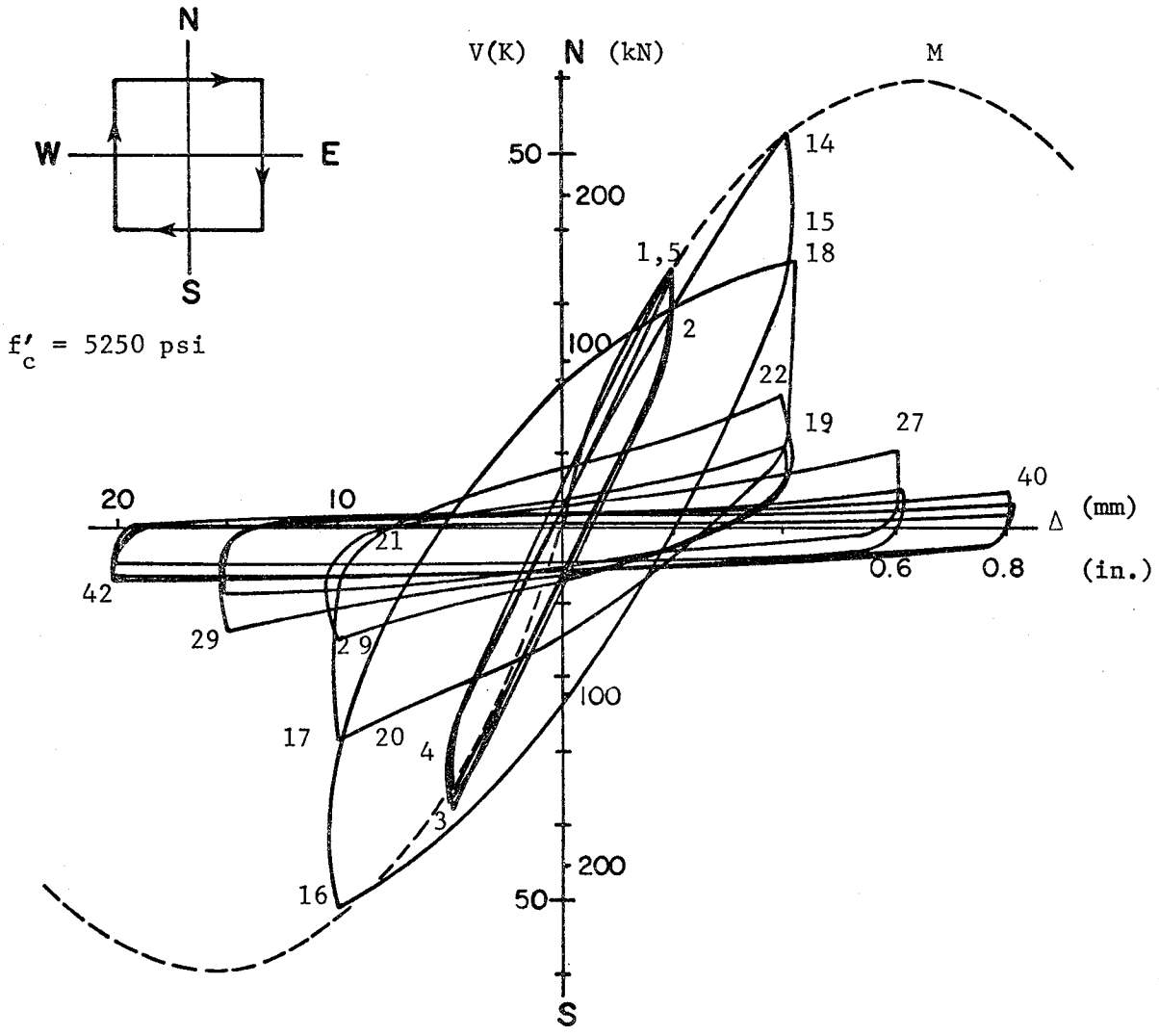

Fig. 5.12 Load-deflection relationship - S (NS direction)

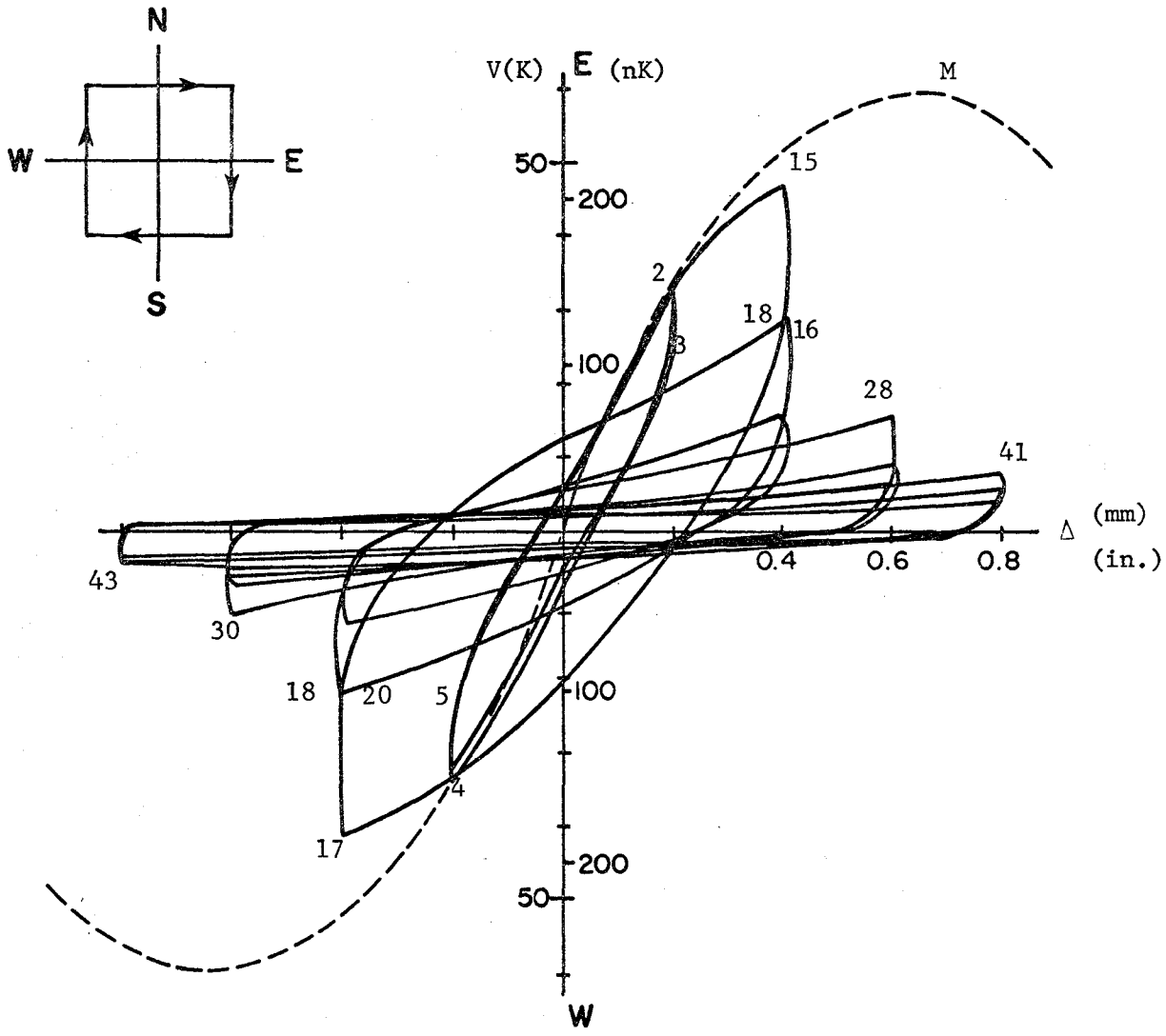

Fig. 5.13 Load-deflection relationship - S (EW direction)

reached, the west deformation is held constant while the NS deformation changes a total of 2Δ ($-\Delta_i$ to $+\Delta_i$, load stage 17 to 18). In Fig. 5.13 the large reduction in shear force from load stage 17 to 18 can be seen. It can be seen that the specimen has virtually no stiffness or strength at deformation levels $3\Delta_i$ and $4\Delta_i$.

The change in force in each direction is shown in Fig. 5.14. Note that at deflection level Δ_i the restoring forces trace a fairly stable square pattern. With increase in the deflection level to $2\Delta_i$, the pattern is a square spiral with steady decrease in shear force in both directions, even though the deformation is held constant. The rapid deterioration of the strength of the specimen is readily apparent.

5.6 Comparison of Loading Histories

Figures 5.15 and 5.16 show comparisons of the shear capacity in both principal directions at the first and last peaks at a given deflection level. The shear capacity is expressed as a nondimensional value where the shear force is divided by the area of the column core and the square root of the concrete strength. In all cases, the loading was applied first in the north direction. The figures provide a quick summary of the load-deflection behavior discussed in previous sections.

In all tests the first peak at Δ_i or $2\Delta_i$ in the NS direction was about equal to the monotonic capacity. With unidirectional cycling, the capacity was reduced. With loading in both directions (B), the capacity was further reduced. With simultaneous loading in both directions (cases S and D), the severe deterioration is quite apparent. The curves clearly show that previous loading in one direction has a detrimental influence on subsequent response in the orthogonal direction.

5.7 Crack Patterns

Cracks were marked on the surface of the specimen at peak load stages of each deflection level. In all specimens the first cracks formed were horizontal flexural cracks at the top and the bottom of the column. Under load reversal, the predominant cracks were diagonal shear

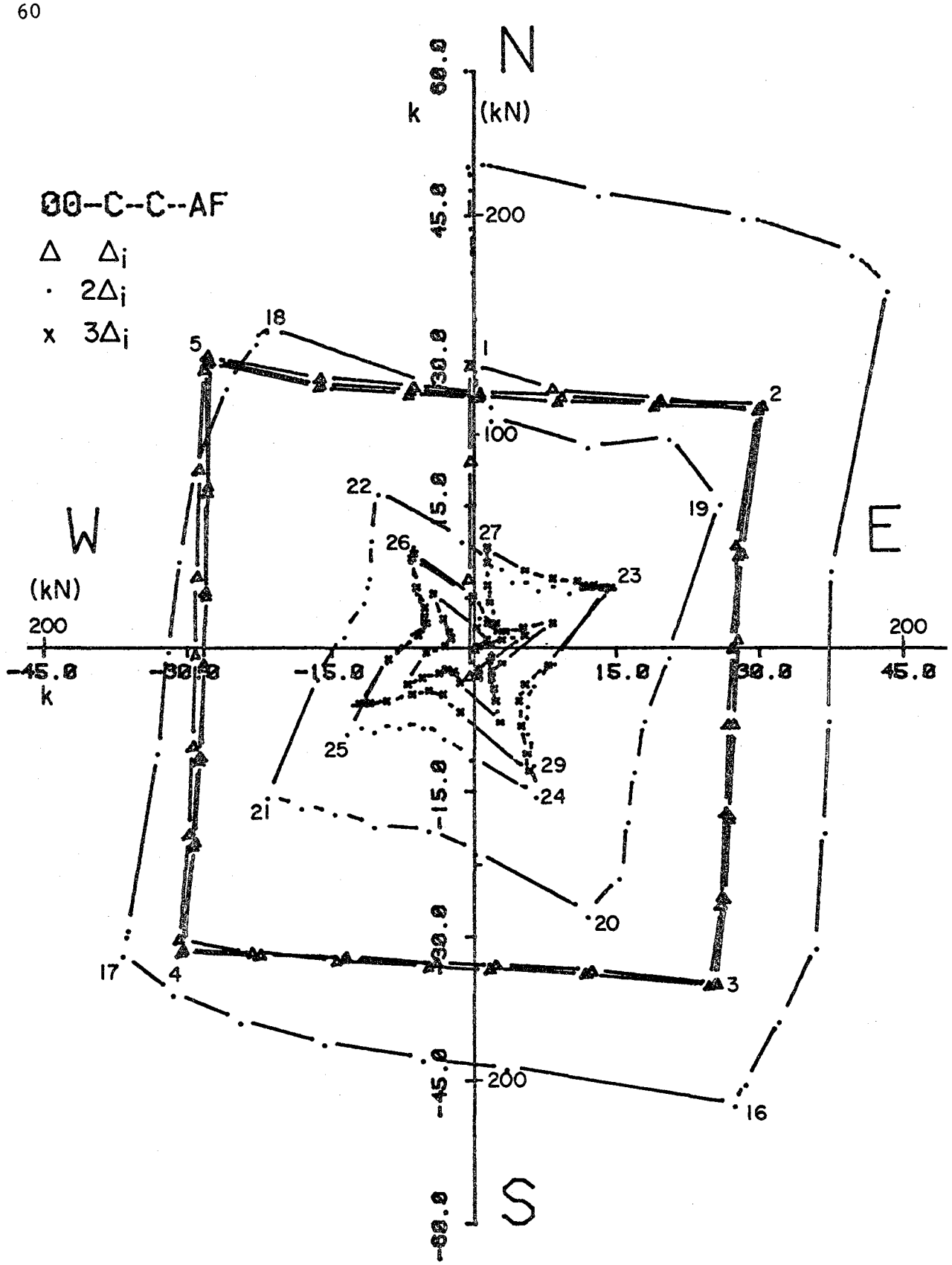

Fig. 5.14 Lateral restoring force, loading history S

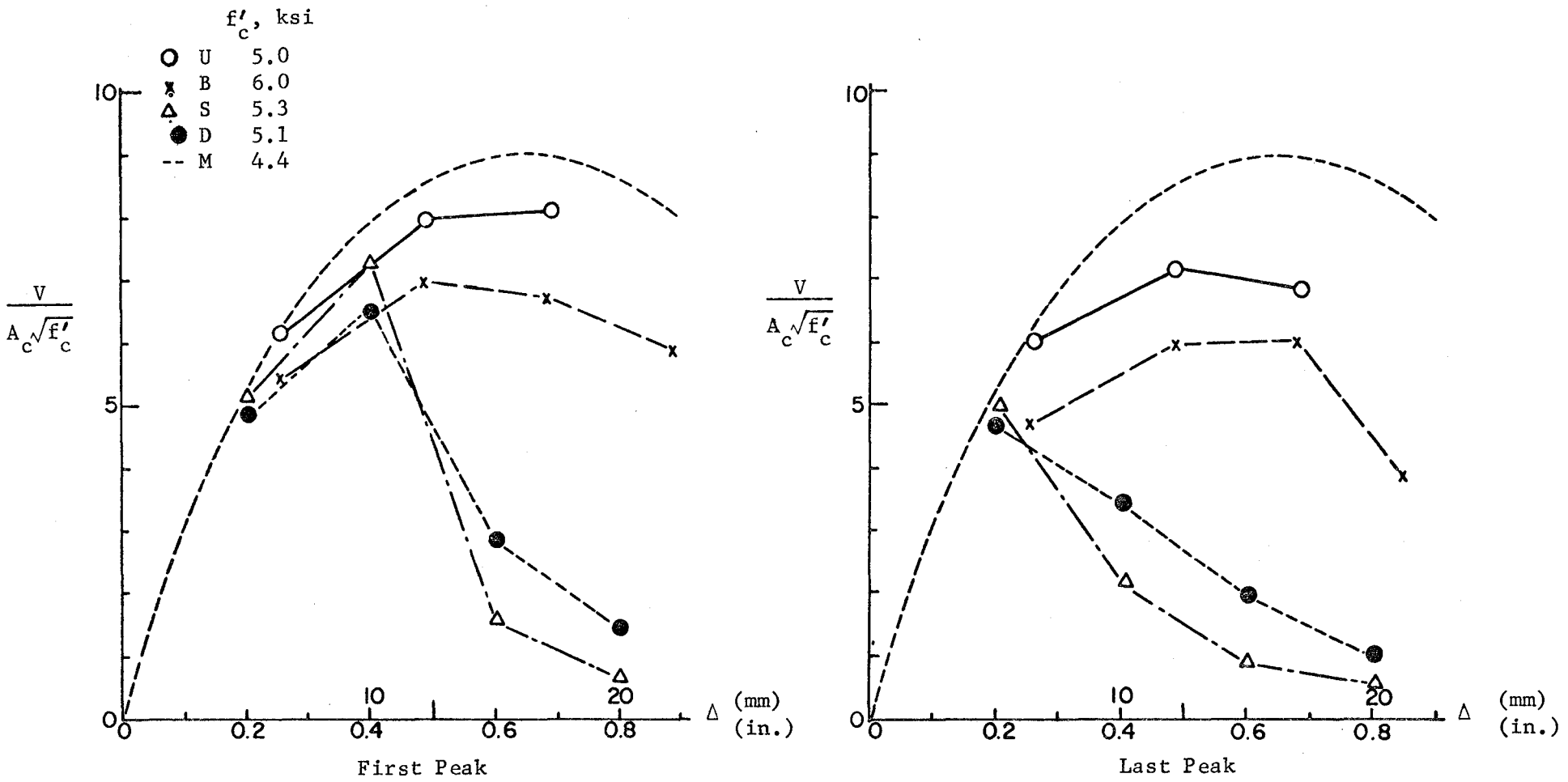

Fig. 5.15 Reduction in shear capacity (NS direction)

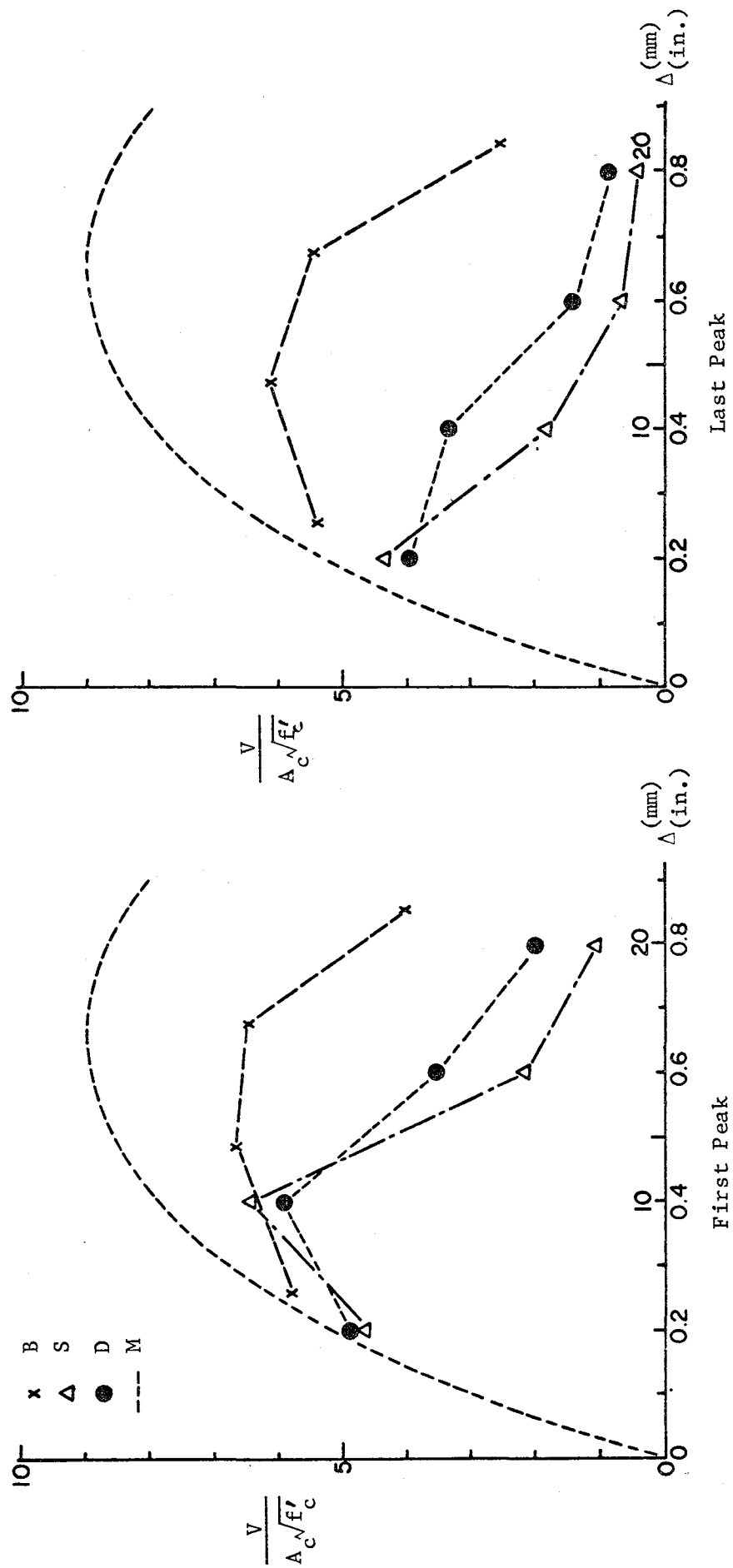

Fig. 5.16 Reduction in shear capacity (EW direction)

cracks. As the deflection level increased, the shear cracks extended and new diagonal shear cracks initiated and propagated toward the mid-height of the column. The shear cracks were almost symmetrically about the center of the column. Near failure, the entire column was cracked and failure was concentrated in several wide cracks. Figure 5.17 shows crack patterns for the four tests.

The crack pattern in the case of unilateral reversals (U) is shown in Fig. 5.17a. Diagonal shear cracks were well-developed and distributed on the two sides which were parallel to the loading direction, and several horizontal flexural cracks were visible on the other two sides.

In the case of alternative bidirectional loading (B), all four sides had diagonal shear cracks, as shown in Fig. 5.17b. The crack pattern on each face is very similar to that of the unilateral loading case.

For the other loading histories, D and S, the final crack patterns are quite similar to that for case B. However, for D and S (Figs. 5.17c and d), the entire surface was covered with cracks after three cycles of load reversals at $2\Delta_i$. For specimen B, cracks propagating the whole surface of the column were not evident until deflection levels of $3\Delta_i$ were reached. In general, the crack patterns indicate the same trends discussed earlier with regard to load-deflection relationships. Loading in both directions simultaneously produced more severe distress than loading in one direction only or alternatively.

5.8 Strains in Transverse Reinforcement

Strain distribution in the transverse reinforcement in the NS direction for the four cases is shown in Fig. 5.18. Each curve represents the strain distribution at the last peak of each deflection level. The strain distribution in the ties coincides with strength behavior discussed earlier. The deterioration of shear capacity is aggravated with bidirectional alternate loading and with loading in both directions simultaneously. Under loading U or B, the most severe shear strength reduction occurred at $4\Delta_i$ deflection level. Under loading S or D, severe shear distress was evident at a $2\Delta_i$ level.

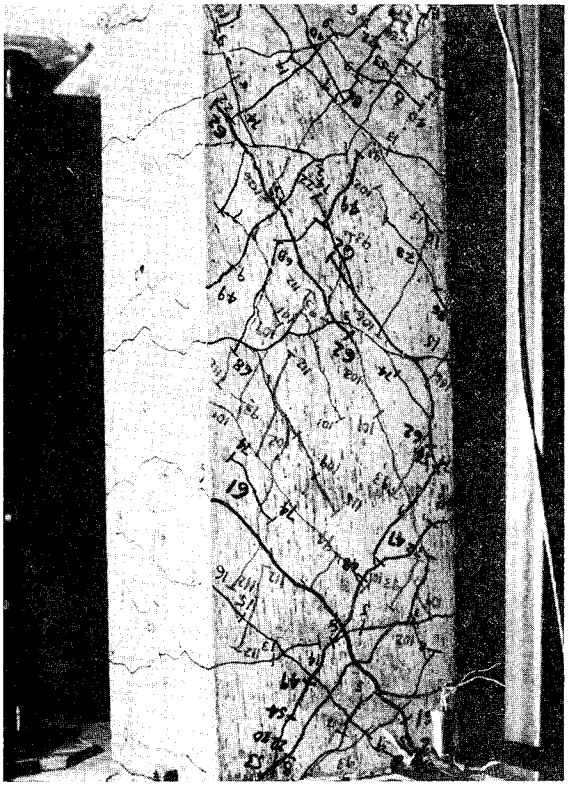

(a) Loading history U

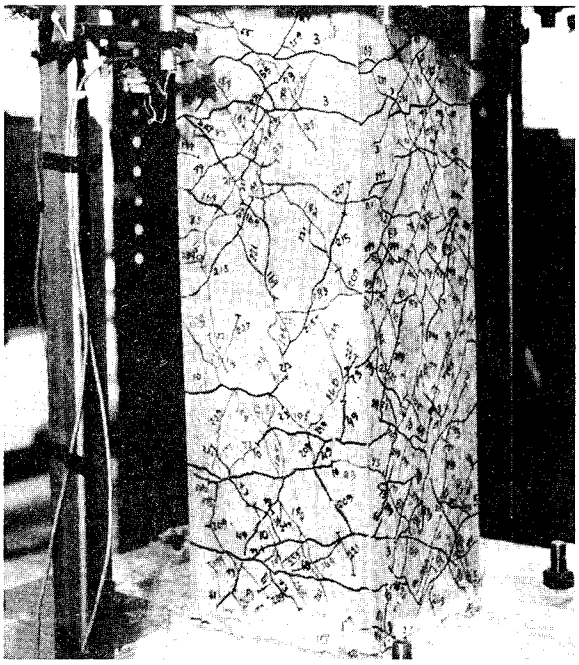

(b) Loading history B

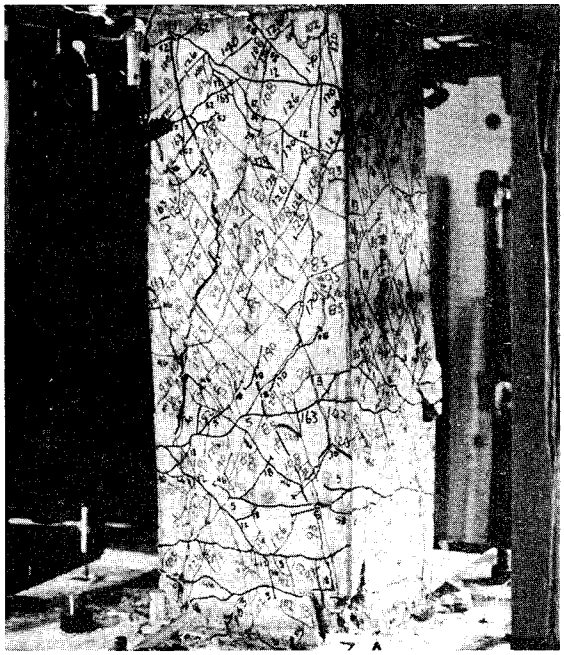

(c) Loading history D

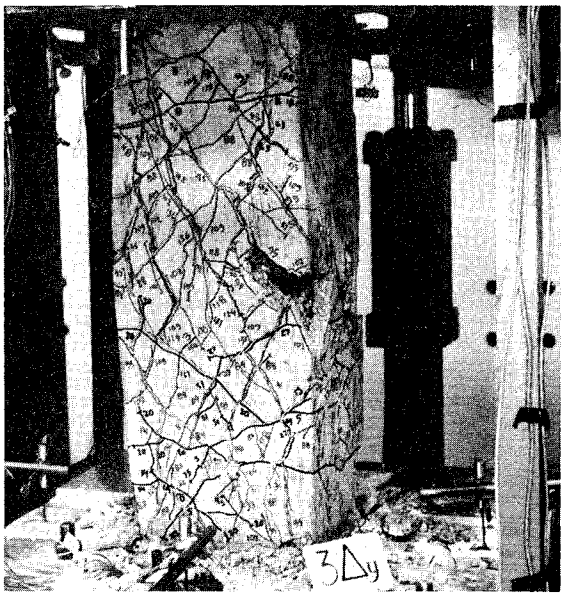

(d) Loading history S

Fig. 5.17 Crack patterns after completion of test

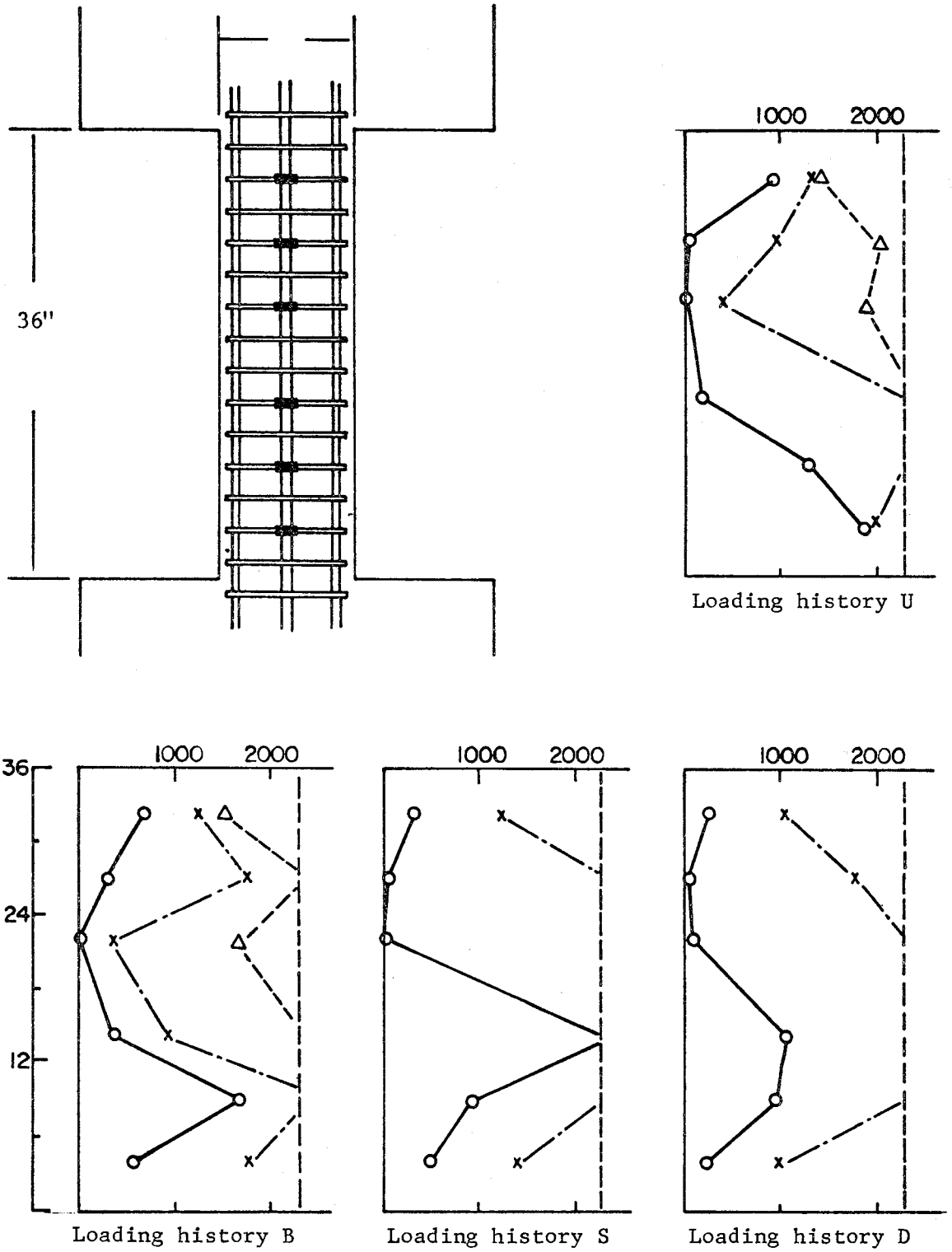

Fig. 5.18 Strain distribution in transverse reinforcement

The same observations can be made on the basis of the transverse steel strain distribution diagrams shown in Fig. 5.18. The distribution pattern for case U is quite similar to that of case B. After three cycles at a $3\Delta_i$ level, almost all ties are at yield. In cases S and D, strains in most ties exceeded yield strain after the third cycle at $2\Delta_i$. In all four cases, nearly all the ties were well below yield at the Δ_i deflection level.

CHAPTER 6

SUMMARY

6.1 Development of Loading and Instrumentation System

In order to apply complex loadings, a number of loading and instrumentation systems were developed. A structural floor-wall system was built which permitted the applied lateral forces to react directly against walls which are monolithic with the floor on which the specimen is anchored. Three-dimensional loading variations can be applied with a servo-hydraulic system and controlled using a minicomputer. The system is capable of applying axial tension or compression to the specimen.

The specimen represents a short column located between stiff floors which remain horizontal during lateral translation. To simulate the end conditions, a hydraulic positioning system was fabricated which permits translation of the specimen in any plane but restrains rotation.

The specimen is a 12x12 in. (31x31 cm) square column with a 36 in. height. The specimen was designed to fail in a shear mode. Loads, displacements and strains were monitored and processed with a computer-controlled data acquisition system.

6.2 Initial Tests

Initial tests using four different loading histories proved the versatility and efficiency of the systems developed. It was possible to program complex loadings and use the computer to control the loads in the three directions simultaneously. The positioning systems effectively restrained rotation and permitted large translations to be applied. Data processing software greatly reduced the time needed to digest the results.

The tests showed that application of load in one direction reduces the shear capacity of the specimen on subsequent application of load in the orthogonal direction. With application of load in both directions simultaneously, the reduction in shear capacity is even more severe. On the basis of the limited tests discussed, it would appear that the loading path is not as significant as the deformation level or relative translation in both directions. It is clear that load history is an important parameter in defining shear capacity of a column.

6.3 Future Study

Work is underway with specimens subjected to other lateral load histories and to varying axial load levels (tension through compression). Based on the entire series of tests, a behavioral model is being developed and the results are being assessed to determine their impact on design recommendations. It is anticipated that a rigorous study of various geometric and loading parameters can be undertaken with the systems developed and the influence of shear deterioration of columns under three-dimensional load variation can be effectively evaluated.

REFERENCES

1. Okada, T. et al., "Analyses of the Hochinohe Library Damage by '68 Tokachi-Oki Earthquake," Proceedings, U.S.-Japan Seminar on Earthquake Engineering with Emphasis on Safety of School Buildings, Sendai, Japan, September 1970, pp. 172-189.

2. Aoyama, H., and Sozen, M. A., "Dynamic Response of a Reinforced Concrete Structure with Tied and Spiral Columns," Proceedings, Fifth World Conference on Earthquake Engineering, Rome, 1973, Paper No. 15.

3. Aktan, A. E., Pecknold, D. A. W., and Sozen, M. A., "Effects of Two-dimensional Earthquake Motion on a Reinforced Concrete Column," Civil Engineering Studies, Structural Research Series 399, University of Illinois, May 1973.

4. Pecknold, D. A. W., and Sozen, M. A., "Calculated Inelastic Structural Response to Uniaxial and Biaxial Earthquake Motions," Proceedings, Fifth World Conference on Earthquake Engineering, Rome, 1973, Paper No. 223.

5. Selna, L. G., Morrill, K. B., and Ersoy, O. K., "Shear Collapse, Elastic and Inelastic Biaxial Studies of the Olive View Hospital Psychiatric Day Clinic," U.S.-Japan Seminar on Earthquake Engineering, Berkeley, 1973.

6. Bresler, B., "Design Criteria for Reinforced Columns under Axial Load Journal of the American Concrete Institute, Proc. V. 57, No. 5, November 1960, pp. 481-490.

7. Fleming, J. F., and Werner, S. D., "Design of Columns Subjected to Biaxial Bending," Journal of the American Concrete Institute, Proc. V. 62, No. 3, March 1965, pp. 327-342.

8. Takizawa, H., and Aoyama, H., "Biaxial Effects in Modeling Earthquake Response of R/C Structures," Earthquake Engineering and Structural Dynamics, Vol. 4, 1976, pp. 523-552.

9. Takizawa, H., "Biaxial and Gravity Effects in Modeling Strong-Motion Response of R/C Structures," Sixth World Conference on Earthquake Engineering, New Delhi, 1977, Paper No. 3-9, pp. 49-54.

10. Takiguchi, K., Kokusho, S., and Ohada, K., "Experiments on Reinforced Concrete Columns Subjected to Biaxial Bending Moments," Transactions of A.I.J., No. 229, March 1975, pp. 25-33.

11. Takiguchi, K., Kokusho, S., and Ohada, K., "Experiments on Reinforced Concrete Columns Subjected to Biaxial Bending Moments--II," Transactions of A.I.J., No. 247, September 1976, pp. 37-43.

12. Takiguchi, K., Kokusho, S., and Ohada, K., "Analysis of Reinforced Concrete Sections Subjected to Biaxial Bending Moments," Transactions of A.I.J., No. 250, December 1976, pp. 1-8.

13. Okada, T., Seki, M., and Asai, S., "Response of Reinforced Concrete Columns to Bi-directional Horizontal Force and Constant Axial Force," Bulletin of Earthquake Research Center, University of Tokyo, No. 10, 1976, pp. 30-36.

14. ACI-ASCE Committee 426, "The Shear Strength of Reinforced Concrete Members," Journal of the Structural Division, ASCE, Vol. 99, No. ST6, Proc. Paper 9791, June 1973, pp. 1091-1187.

15. Mattock, A. H., "Connections in Precast Concrete Buildings Subjected to Earthquake," Proceedings, U.S.-Japan Seminar on Earthquake Engineering with Emphasis on Safety of Reinforced Concrete Structures, Berkeley, September 1973.

16. Building Research Institute, Ministry of Construction, Japan, "A List of Experimental Results on Deformation Ability of Reinforced Concrete Columns under Large Deflection (No. 3)," (in Japanese), Kenchiku Kenkyu Shiryo, No. 21, February 1978.

17. ACI Committee 318, Building Code Requirements for Reinforced Concrete (ACI 318-77), Detroit, 1977.

18. Woodward, Kyle A., and Jirsa, James O., "Design and Construction of a Floor-Wall Reaction System," CESRL Report No. 77-4, Civil Engineering Structures Research Laboratory, The University of Texas at Austin, Texas, December 1977.